DETERMINATION OF LATERAL INFLOWS IN THE KUPARUK RIVER WATERSHED,

A STUDY IN THE ALASKAN ARCTIC

By

Levi D. Overbeck
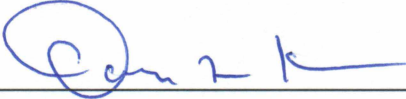
RECOMMENDED: _____

Dr. Horacio Toniolo
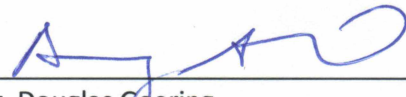
_____

Dr. Svetlana Stuefer

_____

Dr. Douglas Kane
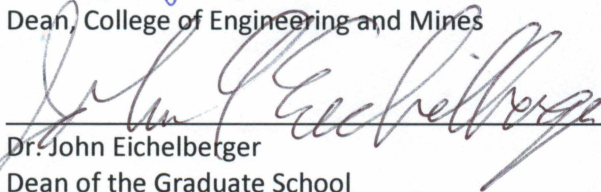Advisory Committee Chair

_____

Dr. Robert Perkins, Chair
Department of Civil and Environmental Engineering
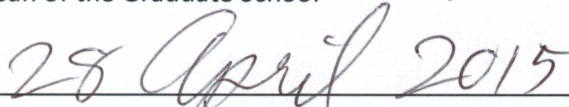
APPROVED: _____

Dr. Douglas Goering
Dean, College of Engineering and Mines

_____

Dr. John Eichelberger
Dean of the Graduate School

_____

Date

DETERMINATION OF LATERAL INFLOWS IN THE KUPARUK RIVER WATERSHED,

A STUDY IN THE ALASKAN ARCTIC

A

THESIS

Presented to the Faculty

of the University of Alaska Fairbanks

in Partial Fulfillment of the Requirements

for the Degree of

MASTER OF SCIENCE

By

Levi D. Overbeck, B.S.

Fairbanks, Alaska

May 2015

Abstract

The objectives of this research were to investigate the relationships between lateral inflows and watershed characteristics within the Kuparuk watershed of Arctic Alaska, as well as to quantify the lateral inflows to be used as an input for calibrating and running a process-based instream water temperature model. Determination of lateral inflows was accomplished by constructing hydrographs at multiple locations along Imnavait Creek and the Kuparuk River using stage and discharge field measurements. The hydrographs were then routed between gauging stations downstream (starting upstream) using the Muskingum routing method; and finally subtracting the routed hydrograph from the downstream measured hydrograph to calculate any additional water that had entered the reach between gauging stations. Results showed, as a general trend, that reaches within the northern foothills of the Brooks Range experienced larger lateral inflow contributions per square kilometer and had larger runoff ratios than subsequent reaches to the north where the terrain flattens out and transitions into the coastal plain. Two reaches within the watershed contradicted the general trend. The low-gradient reach nearest to the Arctic Ocean experienced larger lateral inflows throughout the summer that were unaffected by rainfall precipitation events, this is believed to be caused by snowmelt water initially stored in the low gradient terrain and slowly released into the drainage network during summer months. This area is rich with wetlands, ponds, and lakes and snow-damming during break up is prevalent. The other reach was located upstream of the Kuparuk aufeis field and was observed to lose water during the summer of 2013, supporting a hypothesis that the aufeis formation in this area is fed throughout the winter by a large talik upstream.

Table of Contents

List of Figures

List of Tables

List of Appendices

Acknowledgements

Collection of field data was completed by Levi Overbeck, Joel Homan, Ken Irving, and Robert Geick from the University of Alaska Fairbanks and Bethany Neilson, Tyler King, Noah Schmadel, Milada Majerova, Austin Jensen, and Mitchell Rasmussen from Utah State University. Thank you for all of the time spent in the Alaskan Arctic feeding the mosquitos in order to get the measurements we needed.

I would like to express my gratitude to my advisor Douglas Kane for the opportunity to embark on this research and with the help of my graduate committee Horacio Toniolo and Svetlana Stuefer for the guidance required to complete it. Furthermore I would like to thank Bethany Neilson for all the time and effort put into making this project happen, and for helping me solve problems along the way. To Joel Homan, Tyler King, and Mitchell Rasmussen, the best field teammate's one could ask.

This research would not have been possible without the encouragement, understanding, and compassion of my loving wife, Jacquelyn.

1. Introduction

Over the past century global surface air temperature has risen 0.6 ± 0.2 °C and is expected to continue to rise, the Arctic region is forecasted to experience temperature increases in excess of 40% of the global mean (Houghton et al., 2001). Moisture transportation is also expected to increase along with temperature (Houghton et al., 2001). Between 1936 and 1999 discharge from six of the largest Eurasian rivers into the Arctic Ocean rose by 7% (Peterson et al., 2002), and one model predicts that the average discharge of these rivers could increase up to 48% by 2100 (van Vliet et al., 2013). The same study also determined that average summer water temperature in the same rivers could increase by 2 °C (van Vliet et al., 2013).

The dynamic interactions in the Arctic between temperature increases, changes in precipitation patterns, lengthening of growing seasons, increasing active layer thicknesses, and animal species are not well understood (Hinzman et al., 2005). It is known that changes in instream temperatures have the potential to impact migration and reproduction patterns of aquatic life (Cooter & Cooter, 1990), including both fresh water and near shore marine fish (Wood & McDonald, 1997). Reductions in fish populations inherently have the potential to affect the lives of Alaskans who depend on those fisheries for either employment or subsistence.

To better understand the dominant processes that control instream temperatures, a process-based instream temperature model is under construction by researchers at Utah State University for the streams and rivers of Arctic Alaska. Field data are being implemented into the development, calibration and validation/testing of the model. A conceptual diagram for the model is shown in Figure 1.1.
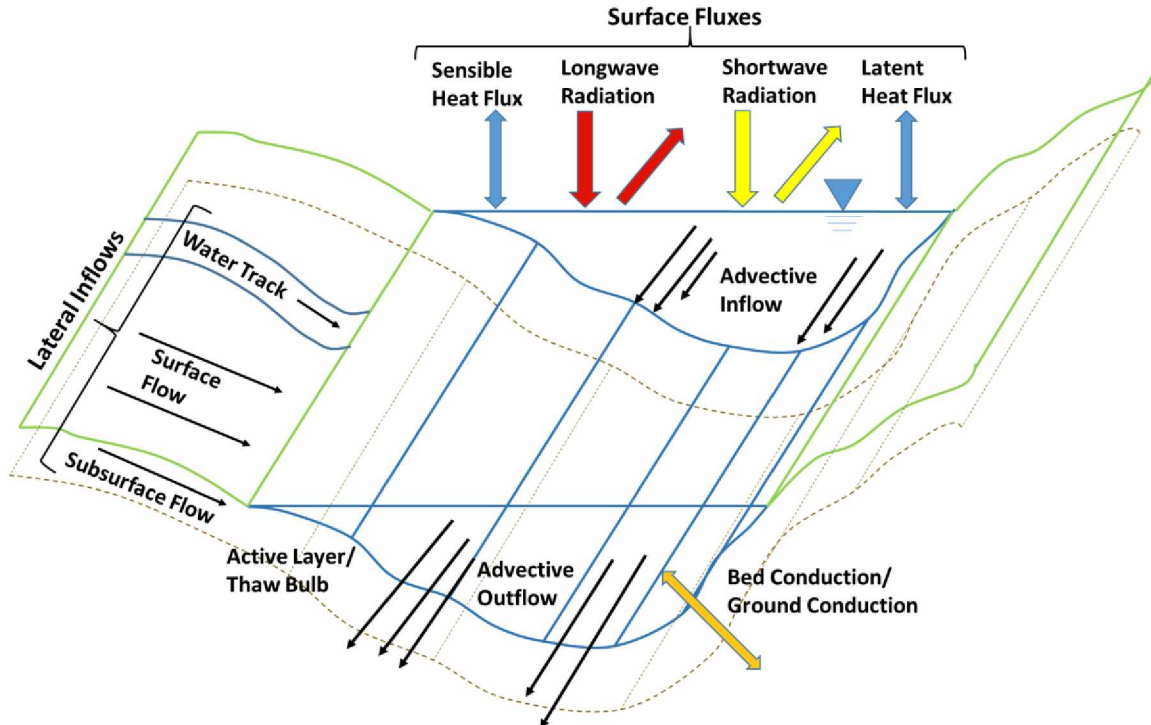
Figure 1.1: Conceptual diagram for the instream temperature model.
Conceptual diagram for the instream temperature model where the black arrows indicate the movement of water and the colored arrows indicate energy transfer.

The model will be used to simulate the possible effects of various changes in climate and hydrology.

Data collection was a collaborative effort between the University of Alaska Fairbanks and Utah State University and included river stage and discharge, instream temperature, incoming and outgoing radiative fluxes, river bed temperature profiling, and precipitation monitoring. From the field data the lateral inflows will be calculated throughout the Kuparuk River watershed and will serve as an important input to the instream temperature model.

1.1 Research Goals

This thesis focuses on the quantification of lateral inflows to various reaches of Imnavait Creek and the Kuparuk River to determine relationships between lateral inflows, precipitation patterns, and watershed characteristics. Lateral inflows are not only a source of additional water within a reach but also transport potentially large quantities of heat into a given reach, thus impacting the stream's thermal regime. Within this project, lateral inflows are the designation given to all additional water

2

entering the reach, including contributions from channel precipitation, hillslope runoff due to overland or subsurface flow, watertracks, and tributary streams.

To quantify the lateral inflows and determine their relationships to precipitation patterns and watershed characteristics, the following steps were taken:

- Stage-discharge relationships were built for each gauging site through the coupling of stage and discharge measurements.

- Hydrographs were calculated for each gauging site through the use of the stage-discharge relationships, known as gauged hydrographs.

- The gauged hydrographs were routed downstream using a variable parameter version of the Muskingum routing method.

- Lateral inflows were determined by subtracting the routed hydrographs from the downstream gauged hydrograph.

- Precipitation records were built for sub watersheds using a simple arithmetic average from Thiessen polygon networks.

- Cumulative lateral inflows were calculated, and normalized by the contributing watershed area for each reach, along with runoff ratio.

2. Background

2.1 Study Area

The Kuparuk watershed is located on the Northern Slope of Alaska, shown in Figure 2.1. The Kuparuk River is fed by numerous tributaries including Imnavait Creek and the Toolik River, in total it drains 8,360 km^2 of the Alaskan Arctic upon reaching the USGS gauging site (USGS gauge site 15896000). The headwaters of both the Kuparuk River and the Toolik River are located in the northern foothills of the Brooks Range, from there they flow northward to their confluence on the coastal plain, where they continue northward to the Arctic Ocean.
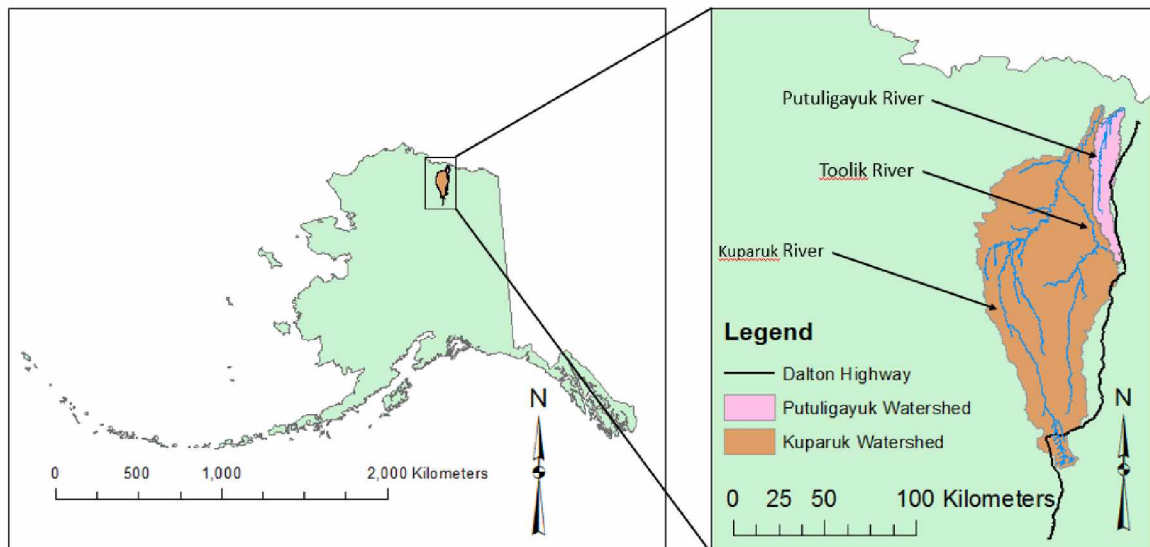
Figure 2.1 Location map of the research area.
Map showing the Kuparuk and Putuligayuk watersheds on the North Slope of Alaska.

The Kuparuk watershed is composed 62% of what is described as foothills (Kane et al., 2008), these glacially carved hills and valleys are vegetated primarily by tussock sedge tundra but also by lichens, dwarf willows, and dwarf birches (Walker et al., 1989). Moving north toward the coastline the terrain becomes much flatter giving way from hills to thaw lakes in a landscape that was never glaciated (Walker et al., 1989). The entire watershed is underlain by continuous permafrost ranging in thickness from 250 m near the foothills to over 600 m thick in the areas around the coast (Osterkamp & Payne,

5

1981). The surface generally remains frozen from October until mid-May, with the active layer only

penetrating 25-40 cm below the surface during the summer throughout the majority of the tundra,

however thaw depths in excess of 100 cm have been measured beneath watertacks (Hinzman et al.,

1991) and areas of well-drained soils.

Investigations into the hydrology of the Kuparuk River, Imnavait Creek, and the Upper Kuparuk

date back to 1971, 1986, and 1993, respectively (Kane et al., 2008). Initially investigations focused on

measuring annual precipitation totals and determining discharges during peak runoff events with an

emphasis on snowfall and snowmelt runoff. Annual precipitation ranges from 193 mm near the coast to

334 mm in the foothills (Kane et al., 2014). Of the annual precipitation within the watershed 30-40 % is

in the form of snow, two-thirds of which leaves as runoff during spring break up (Kane et al., 2008). The

spring break up usually occurs within a period of two weeks or less (McNamara et al., 1998). For most

basins within the arctic, snowmelt produces the annual peak flood event and for larger basins it is also

responsible for the record flood. However, for small and intermediate basins within the foothills the

record flood is more likely to be caused by a summer precipitation event that can blanket the entire

basin (Kane et al., 2008).

Water balances conducted on the whole Kuparuk River as well as on the Upper Kuparuk and

Imnavait Creek found summer precipitation had an average rainfall runoff ratio of 0.35, 0.65, and 0.45

respectively (Lilly et al., 2000). Investigations into Imnavait Creek revealed that after extended periods

of drought approximately 15 mm of rainfall was required before the hillslopes would begin producing

runoff (Kane et al., 1989) and an increase in stream flow was observed. Runoff throughout the Upper

Kuparuk and Imnavait Creek was observed to move downslope primarily though the upper organic layer,

which ranges in thickness from 5 cm along the ridges to 20 cm near the valley bottoms (Hinzman et al.,

1993). The hydraulic conductivity within the organic layer ranges from 10-100 times greater than that of

the underlying mineral soil (Hinzman et al., 1991). Due to the high hydraulic conductivity of the organic

6

layer, surface runoff rarely occurs due to rainfall rates exceeding infiltration rates, but instead occurs

when the organic layer becomes saturated (Kane et al., 1989). As summer progresses and the active

layer increases in depth more of the soil profile contributes to runoff leading to longer recession periods

after storm events (Hinzman et al., 1991). During the growth of the active layer it has been observed

that the melt water within the soil has little or no contribution to stream flow (Kane et al., 1989).

Hydrologic studies of the coastal plain region have mainly been conducted within the

neighboring watershed of the Putuligayuk River, shown in Figure 2.1, a catchment confined solely to the

coastal plain. The Putuligayuk River watershed is adjacent to the East side of the Kuparuk watershed

and has an area of 471 km^2 (Bowling et al., 2003). Within this low gradient watershed precipitation

events occurring after spring break up were followed by little to no discernable streamflow response.

This was caused by a disconnection in the drainage network induced by the low gradient terrain which

lead to greater evaporation than precipitation (Bowling et al., 2003).

Located within the Kuparuk watershed is an aufeis field, shown in Figure 2.2, an ice sheet that

forms throughout the winter from groundwater flowing up to the surface where it freezes. The ice

initially freezes and fills in the river channel, as the winter progresses the water continues to flow out of

the ground and over the ice forming thicker layers while also expanding the ice sheet both downriver

and laterally out into the floodplain (Yoshikawa et al., 2007). A ten year study (Yoshikawa et al., 2007) of

the Kuparuk aufeis field from 1996 to 2005 using SAR analysis estimated that the average maximum

volume of ice is roughly 23,384,000 m^3 and estimated that the aufeis comprised 27-30% of the annual

groundwater discharge from the nearby spring. The potential size of aufeis fields makes them the

second largest temporary storage of fresh water behind the snow cover in unglaciated basins (Kane &

Slaughter, 1972).
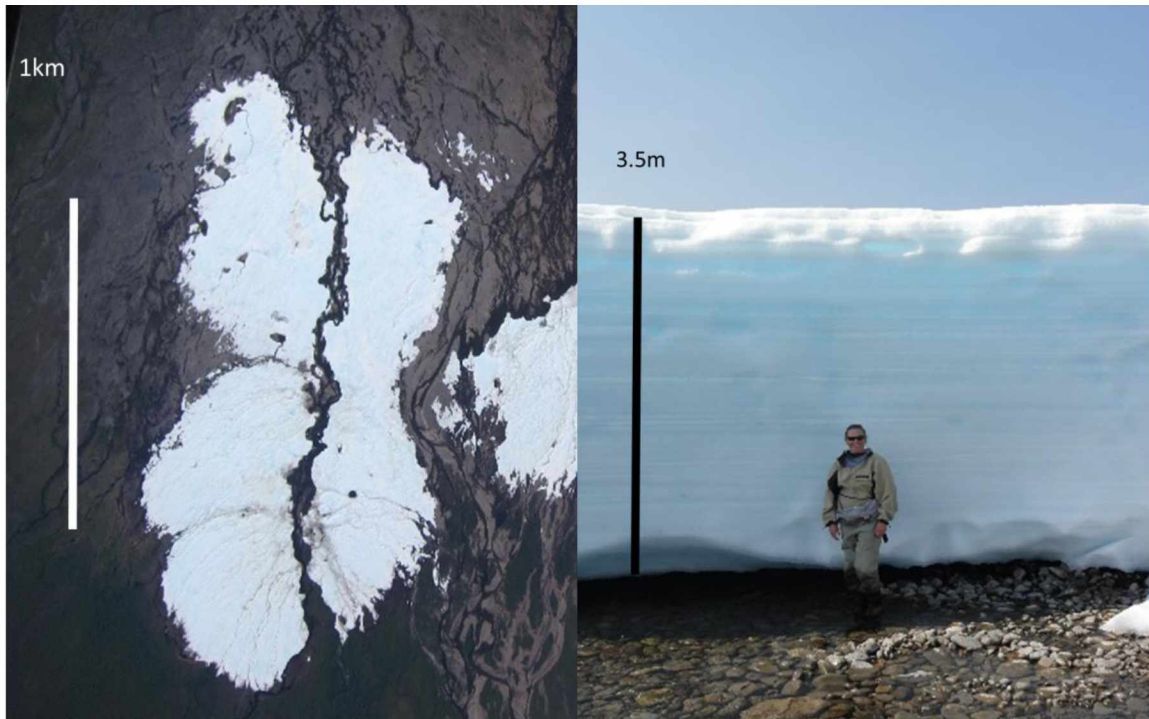
Figure 2.2 Images of the Kuparuk aufeis.
     Areal photo of the Kuparuk aufeis field taken using Utah State University's AggieAir payload
     mounted on a helicopter on August 6, 2013 (left), Bethany Neilson next to the Kuparuk aufeis
     during June 2013 (right).

Many aufeis fields within the arctic are fed by springs emitting from subpermafrost groundwater

(Kane et al., 2013). Comparisons of water temperature and chemical composition between the spring

feeding the Kuparuk aufeis and other springs found throughout the North Slope suggest that the source

for the Kuparuk aufeis is not subpermafrost but instead a near surface talik below the river (Yoshikawa

et al., 2007). The Kuparuk River has been observed to lose water and occasionally run dry both

immediately above the aufeis field as well as farther up river in the foothills (Betts & Kane, 2015 In

Press). It is hypothesized that water lost from the Kuparuk River recharges a near surface talik that

supplies water to the spring feeding the Kuparuk aufeis in winter.

2.2 Site Selection

Gauging sites throughout the Kuparuk watershed at which field measurements were made were

chosen to isolate variations in watershed characteristics, to provide a variety of spatial scales, and to

utilize gauging locations already in operation. The drainage areas for the subwatersheds are shown in

Table 2.1; for the location of the individual gauging sites throughout the watershed for 2013 and 2014 see Figure 2.3 and Figure 2.4 respectively.

Table 2.1: Drainage areas for the subwatersheds gauged in 2013 and 2014.

Sub-Watershed	Area (km^2)
Above Kuparuk River Stilling Well (Upper Kuparuk)	133
Above Imnavait Creek Weir	2.1
Imnavait Creek Weir to Imnavait Creek Confluence	15.2
Kuparuk River Stilling Well to Site 8	56.6
Site 8 to Site 7	38.4
Site 7 to Site 5	306
Site 4 to Site 3T	1210
Site 3T to Site 2A	2350
Site 4 to Site 3B	2570
Site 3B to Site 2A	1433
Toolik River Watershed	2840
Site 2A to USGS Gauging Site	986

Subwatersheds Gauged within the Kuparuk Watershed During the 2013 Field Season
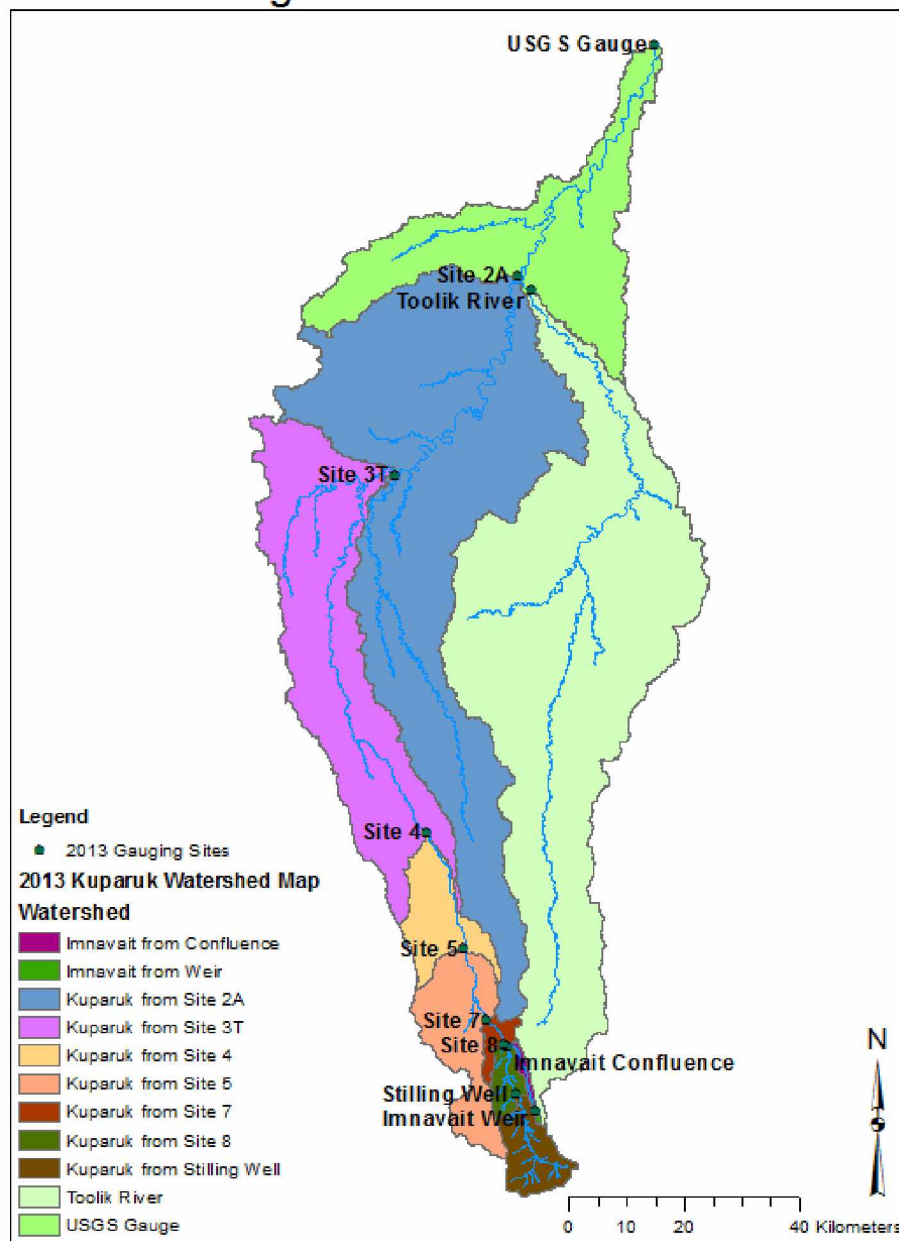
Figure 2.3 Watershed map showing instrumented sites in 2013.
Map of the Kuparuk watershed showing the 2013 gauging locations and the extent of the contributing area for those gauging locations.
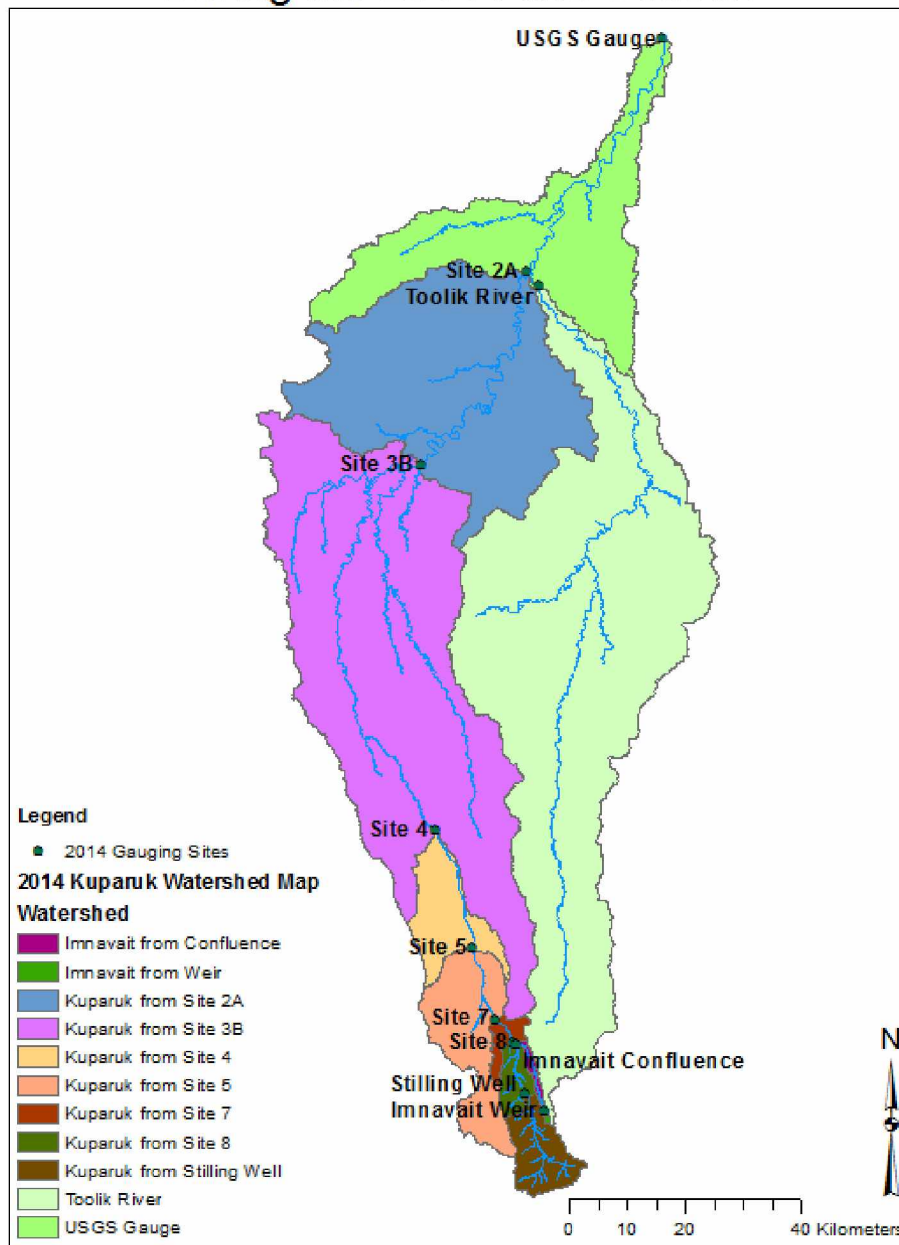
Figure 2.4 Watershed map showing instrumented sites in 2014.
Map of the Kuparuk watershed showing the 2014 gauging locations and the extent of the contributing area for those gauging locations.

The Kuparuk River stilling well site and Imnavait weir site (the two southernmost sites) are long-term flow monitoring stations operated by the Water and Environmental Research Center (WERC) at the University of Alaska, Fairbanks. The site of for the stilling well is a straight section of the Kuparuk River located within walking distance of the Dalton Highway that allows for convenient discharge measurements to be made at both low flow and high flow conditions. The watershed area upstream of this site referred to as the area above the Kuparuk stilling well in this paper is also referred to as the Upper Kuparuk earlier in the text. At the Imnavait weir site, a compound weir consisting of a V-notch for low flow conditions and trapezoidal sides for medium and high flow conditions has been installed with wing walls extending out laterally as well as down into the active layer in order to concentrate the flow through the weir opening (Figure 2.5). The USGS Kuparuk River gauging site was used to mark the northernmost extent of the Kuparuk watershed, near where the river drains into the Arctic Ocean. It was beneficial to use the site gauged by the USGS as access to the Kuparuk River is restricted due its location on the Prudhoe Bay oil-field. Further, the river at this location is a challenge to gauge, even at low flow conditions, without the use of a motorized vessel.

Figure 2.5 Images of the Imnavait Creek weir.
    The weir on Imnavait Creek is shown from upstream at medium flow conditions (left) and from downstream at low flow conditions (right).

Proceeding northward from the Kuparuk River stilling well and Imnavait weir, site 8 was located approximately 8.3 km north of the Dalton Highway just below where Imnavait Creek joins the Kuparuk River. Imnavait Creek was gauged upstream of the confluence in order to avoid any possible effects from backwater, providing an opportunity to investigate inflows on a smaller stream as well as to isolate the Kuparuk River between the stilling well and site 8. Site 7 was chosen 5.1 km to the north-west of site 8 to provide a shorter, more intensive study reach, where river and tributary temperatures could be more closely investigated for the energy balance model. Site 5 was 13 km north of site 7 and south of the aufeis field; it was intended to avoid locations where the river had been observed to significantly lose water and go dry in previous years.

Site 4 is located 21 km north of site 5 where the various braided streams emerging from the aufeis field have come back together. Site 4 works as a reset point within our investigation, a point for which no upstream data are available due to a lack of understanding of the processes surrounding the aufeis field. Site 4 also marks the beginning of the physiographic transition out of the foothills and onto the coastal plain. Site 3T (also known as OKB for the instream temperature model and located within the main channel of Kuparuk) was initially located 62 km north of site 4 in 2013 before being shifted an additional 4.0 km downriver in 2014 and becoming site 3B. The shift moved the gauging site from upriver (above) to downriver (below) of the confluence with what we refer to as the White Hills River. The relocation of site 3T to 3B in 2014 significantly increased the drainage area by incorporating the White Hills River into the subwatershed. This new 3B subwatershed has similar characteristics to that of 3T and clearly separates the land downstream of the confluence which has a significantly lower hydraulic gradient.

Site 2A was located on the Kuparuk River just upriver of the confluence with the Toolik River, 38 km north-east of site 3B and 47 km south-west of the USGS gauging site. The Toolik River was also gauged near the confluence to isolate the coastal plain between site 2A and the USGS site as well as

enable possible comparison at the watershed scale between the Toolik watershed and the Kuparuk watershed. During the 2013 field season a very limited amount of data were collected for the Toolik River, this was due to trouble isolating the main channel, a problem caused by the river being near flood stage at the time of initial installation. As a result the lateral inflows between the confluence of the Toolik River with the Kuparuk River and the USGS gauging site could not be determined in 2013.

2.3 Muskingum Routing

In order to compare the upstream hydrograph to the downstream hydrograph and determine the lateral inflows within a reach, the upstream hydrograph was first be routed through the reach. Of the available methods to route flows through a reach, a variable parameter version of the Muskingum method was selected based on the limited availability of data for the selection of physical parameters of each reach.

The Muskingum method was developed by McCarthy around 1934 as a linear time-invariant system for routing flood waves (Guang-Te & Singh, 1992). The Muskingum method relates the storage (w) within a river reach to the inflow (I) and outflow (O) of the reach using two parameters, K representing the travel time of the reach and X a weighting factor for attenuation (Guang-Te & Singh, 1992):

$$w = K[X * I + (1 - X) * O] \qquad \text{Eqn (1)}$$

In a simplified form solved for the outflow, Equation 1 can be represented as (Guang-Te & Singh, 1992):

$$O_{(i+1)} = C_1 * I_{(i+1)} + C_2 * I_{(i)} + C_3 * O_{(i)} \qquad \text{Eqn (2)}$$

where i indicates the timestep and the coefficients C_1, C_2, and C_3 can be calculated using the timestep size of the inflow hydrograph (Δt) via (Guang-Te & Singh, 1992):

$$C_1 = \frac{0.5 * \Delta t - K * X}{0.5 * \Delta t + (1 - X) * K} \qquad \text{Eqn (3)}$$

$$C_2 = \frac{0.5 * \Delta t + K * X}{0.5 * \Delta t + (1 - X) * K} \qquad \text{Eqn (4)}$$

$$C_3 = \frac{-0.5 * \Delta t + (1 - X) * K}{0.5 * \Delta t + (1 - X) * K}$$ Eqn (5)

The sum of $C_1, C_2,$ and C_3 should equal to 1. This method is implemented by dividing a river

reach into several segments and routing the upstream hydrograph down river one segment at a time.

The number of segments used can be used as a calibration tool, along with K and X, but is subject to the

stability requirement (Lawler, 1964):

$$2 * K * X < \Delta t \leq K$$ Eqn (6)

Traditionally K and X were assumed to be constant between segments and timesteps, an

assumption that holds true if the storage-flow is linear (Guang-Te & Singh, 1992). Realistic values of X

have been shown to vary between 0 and 0.5, where a value of 0.5 provides equal weight to inflow and

outflow and a value of 0 simply translates the wave downstream (Bedient et al., 2013), with values for

natural streams ranging from 0.1 to 0.3 (Wurbs & James, 2002). In the past, values for K and X have

been determined though calibration by matching the routed hydrograph from a known inflow

hydrograph to a measured outflow hydrograph using trial and error, a least squares method (Gill, 1978),

or graphically (Bedient et al., 2013). Most natural systems do not have a linear relation between storage

and flow, for these situations K and X must be varied as the flow varies. An early method to account

for changing values of K and X was the segmented curve method, in which the flow was divided into

subgroups based on the magnitude of the discharge, each subgroup then had different values for

K and X that were applied when flows were within that subgroup (Gill, 1978). Values of the parameters

were also derived using physical characteristics of the reach from the St. Venant equations such that

(Cunge, 1969; Guang-Te & Singh, 1992):

$$K = \frac{\Delta x * A}{\beta * Q}$$ Eqn (7)

$$X = \frac{1}{2} * \left(1 - \frac{q}{S_o * c * \Delta x}\right)$$ Eqn (8)

where Δx is the length of the river reach, A is the channel area, β is an exponent, Q is total discharge, q

is unit discharge, S_o is the channel bed slope, and c is the wave celerity.

This project uses an approximation of the values for K, such that:

$$K = \alpha * Q^{\gamma}$$ Eqn (9)

where Q is the discharge, and α and γ are constants that vary between river reaches. For this project X was selected to be a value of 0.25 whenever possible as recommended for natural systems (Wurbs & James, 2002). To confirm the validity of this method, the routed hydrograph produced using the Muskingum method for several of the river reaches was compared to a routed hydrograph for the same section determined using a kinematic wave model (personal communication, Bethany Neilson, Utah State University).

3. Field Measurements

To determine the lateral inflows along various reaches of the rivers within the Kuparuk watershed, ten seasonal monitoring stations were deployed over the summer of 2013 and 2014. At each of these monitoring stations continuous measurements of river stage were recorded and multiple point discharge measurements were taken throughout both summers to create a stage-discharge relationship and convert the time dependent river stage into discharge. To relate river conditions to rainfall events throughout the summer, precipitation data were collected at several seasonal monitoring stations as well as from preexisting meteorological stations.

To enable the analysis of this research, the following measurements were made as described in more detail in the following sub-sections:

- Precipitation.

- River Stage.

- Discharge.

- Surveys of Pressure Transducer Height.

3.1 Precipitation

Summer precipitation was measured at 8 sites in 2013 and 7 sites in 2014 within the Kuparuk watershed as well as at the nearby Franklin Bluffs meteorological site located on the coastal plain in the adjacent Sagavanirktok River watershed. Precipitation was measured at each site using one of two types of tipping buckets, either the Texas Electronics TE525WS or the TE525MM, connected to a data logger. The gauges function by funneling precipitation to a tipping bucket that tips over when full, emptying itself and sending an electronic pulse that is recorded by the data logger. The TE525WS model features a 20.3 cm (8 in) diameter funnel collector which drains into a tipping bucket that holds 0.254 mm (0.01 in) of water, while the TE525MM model features a 24.5 cm (9.65 in) diameter collector and a tipping bucket that holds 0.1 mm (0.004 in) of water (Figure 3.1).

Figure 3.1 A TE525MM tipping bucket surrounded by a metal alter shield.

The tipping buckets were generally installed at a height between 0.7-1.0 m off the ground attached to a singular supporting rod and surrounded by a metal alter shield. Potential sources of systematic error include undercatch due to: wind, evaporation and wetting losses, and trace events that contained precipitation at a level not significant enough to fill the tipping bucket (Yang et al., 1998). Insufficient data were available at all sites to correct for these errors, so for consistency no corrections were made. The tipping buckets were also observed to deviate from level during the year due to freeze/thaw within the active layer.   All rainfall gauges were equipped with the alter shield to reduce uncertainty associated with gauge undercatch due to wind.

3.2 River Stage

The river stage, or water level, was recorded at monitoring stations throughout the watershed for the Kuparuk River, Imnavait Creek, and the Toolik River as shown in Figures 2.1 and 2.2. Preliminary locations were selected as previously described in site selection. The exact locations for equipment installation were selected so that the river was channelized into a single channel with no bends immediately upstream or downstream, where discharge measurements could be performed during both high-flow and low-flow conditions, and to minimize potential risk to the pressure transducers from debris within the river.

River stage was monitored at the Kuparuk River stilling well and Imnavait Creek weir in 2013 using two Global Water WL400 Series vented pressure transducers at each location. The pressure

transducers at the Imnavait Creek weir were located inside a corrugated metal stilling well that was hydraulically connected to the creek to maintain the position of the pressure transducer and minimize surface undulations of the water. The pressure transducers located at the Kuparuk River stilling well were initially deployed with one pressure transducer within a corrugated metal stilling well and the second within a protective metal sleeve secured to a plate weight with the purpose of holding its position on the bottom of the river. During the summer of 2013 a large precipitation event washed out the stilling well and its corresponding pressure transducer, which was subsequently replaced by a second pressure transducer in a protective metal sleeve secured to a plate weight. During both years the plate weights were not observed to move. At each site both of the pressure transducers were connected to a single data logger that converted electrical current into river stage, readings were taken once every minute and averaged over 15 minute periods.

During the 2014 field season, river stage at the Imnavait Creek weir was measured using a Hobo U20 water level logger pressure transducer located within the corrugated stilling well. The Hobo U20 took a pressure reading once every minute and recorded the 15 minute average. The Hobo U20 water level logger is not vented and therefore had to be adjusted to account for variations in atmospheric pressure. This was done using a BaroTROLL 15psi data logger from In-Situ Inc. that took and recorded a singular measurement every 30 minutes.

For both the 2013 and 2014 field seasons the water level at the confluence of Imnavait Creek with the Kuparuk River was measured and recorded using a YSI 600LS Sonde equipped with a vented cable. The YSI 600LS was attached to a piece of rebar driven into the creek bottom to hold it in place. River stage was measured every minute with the average being recorded every 15 minutes.

At the remaining sites in 2013 and then also including the Kuparuk River stilling well in 2014 river stage was recorded using a Campbell Scientific CS451 pressure transducer with a vented cable connected to a data logger. The pressure transducers were installed within a pvc housing for protection

that was then attached to a studded T-Post driven into the river bottom to hold it in location (Figure

3.2). At all locations, readings were taken at 1 minute intervals but recording averages varied between

15 minute and 30 minute time intervals.

Figure 3.2 Sensor instalation on the Kuparuk River.
    A pressure, temperature, and conductivity sensor secured within the pvc housing (left) which is
    then secured to a t-post in the river (right).

3.3 Discharge

Discharge measurements were made periodically at every location where pressure transducers

were installed to build a stage-discharge relationship and enable the conversion of the continuous stage

measurements into a hydrograph for each site. The timing and number of discharge measurements at

each site varied, but an effort was made to collect discharges across the full range of stages witnessed;

however, measurement opportunities were often affected by the availability of helicopter support to

reach sites, plus weather restricting travel. Special effort was made to obtain measurements at high-

flow and low-flow conditions as discharges outside of the measured bounds would have to be extrapolated by extending the rating curves which could induce additional error.

The method of measuring discharge was determined at each site depending on the flow conditions and channel bathymetry. Whenever possible, the discharge was measured using an Acoustic Doppler Current Profiler (ADCP) or more specifically, the StreamPro from Teledyne RD Instruments, as the StreamPro is able to take significantly more measurements across the transect as well as throughout the water column. However during lower flow conditions the river was often not deep enough for the StreamPro to operate, at which point discharge measurements were taken using an Acoustic Doppler Velocimeter (ADV). This was done using the FlowTracker Handheld ADV from SonTek coupled with a top setting rod. In instances of smaller cross sections and/or significantly low flows, as were present at the Imnavait Weir, a USGS Pygmy Meter was used in conjunction with a digital readout and top setting rod.

Discharge measurements taken using the StreamPro ADCP were done in one of two ways. For deeper and wider river sections the StreamPro was mounted to an inflatable kayak and paddled across the river. For narrower transects a tagline was erected and the StreamPro was shuttled back and forth across the channel mounted on a Tri-Maran, a 3 pontoon hard plastic boat, tethered to the tagline. The two methods are shown in Figure 3.3.

Figure 3.3 The two methods of taking a measurement with the StreamPro.
Tyler King paddles the StreamPro across the river while Levi Overbeck operates the laptop on the far bank (left) and the Tri-Maran tethered to a tag line (right).

Before any measurements were made, the ADCP diagnostic and quality tests were performed as well as a compass calibration. The StreamPro was shuttled across the channel once measuring the depth and velocity to determine the maximum water depth and maximum water velocity which were used to adjust the settings before any measurements were recorded. Measurements were then made utilizing the bottom tracking feature as GPS tracking was not an option. A minimum of four transects were recorded at each site consisting of two in each direction across the river to detect any directional bias in the measurement. During the measurement process the coefficient of variation (standard deviation/mean) was used to gauge the overall quality of the transects measured. If the coefficient of variation was greater than 5% additional transects were measured (Turnipseed & Sauer, 2010). After transects were recorded a moving bed test was performed to detect, and enable if necessary, any adjustments required for sediment transport along the river bottom affecting the StreamPro's performance. After a measurement was completed the files were reviewed for quality control. During the review, the ADCP settings were audited and individual transects were evaluated for bad or missing data as well as ratio of measured to estimated flow. Transects were also compared to one another for consistency in width, area, discharge, and flow direction. Afterwards the mean discharge of the accepted transects was used.

Velocity measurements were performed using the FlowTracker, shown in Figure 3.4, and the USGS pygmy meter; discharges were calculated using the Velocity-Area Method. The velocities used in the calculations were a singular measurement consisting of a 60 second average from 0.6 depth (D) down from the surface if the depth was below 0.75 m or the average of two measurements made at 0.2 D and 0.8 D if the depth was equal to or greater than 0.75 m. Measurements were made spanning the channel at intervals in the attempt to restrict the flow corresponding to each measurement to less than 5% of the total discharge.

Figure 3.4 Velocity measurement using the Flow Tracker.
Levi Overbeck (left) and Tyler King (right) perform a velocity measurement using the Flow Tracker on the Kuparuk River.

3.4 Surveying and Field Measurements of Pressure Transducer Height

Pressure transducer height was surveyed during both years in relation to local temporary benchmarks. In 2013, they were surveyed using a transit, and in 2014 using a Trimble m3 Total Station. Field measurements of the pressure transducers included top-down measurements, where a wooden tape measure was used to measure from the water surface or top of a support down to the top of a sensor head. These measurements were used to adjust the stage record and account for adjustments in the pressure transducers location during a field season.

4. Analysis

4.1 Hydrograph Creation

The first step in creating the seasonal hydrographs for each site was to review and adjust the river stage records so that all stage readings were relative to a single datum. Adjustments to the stage record became necessary any time the pressure transducer was moved during a field season as well as from year to year. Movement of the pressure transducers occurred for a multitude of reasons including but not limited to: adjustment for changes in water level, the need to replace batteries, or debris within the river had shifted or broken the support that held the pressure transducer in place. Adjustments were determined through the use of the river stage record itself as well as through surveying and top down measurements made before and after shifting of the pressure transducer.

For each site, a stage-discharge relation was developed by plotting the measured discharges as a function of river stage at the time of the measurement and then fitting the points with a power function (Linsley JR. et al., 1975) of the form:

$$Q = \Omega * S^{\eta}$$
<div align="right">Eqn (10)</div>

where Q is the predicted discharge, S is the final adjusted stage, and Ω and η are constants. When multiple years of corrected stage data were present for a single site, subsequent years were shifted so stage values would correspond to the initial year's datum through the use of an additional offset. This offset was determined using:

$$\text{Offset} = \frac{\sum_i^n (ST_i - SC_i)}{n}$$
<div align="right">Eqn (11)</div>

where ST is the river stage value during the year to be adjusted, SC is the river stage calculated using the stage-discharge relationship of the previous year, and n is the number of measurements being used in the determination of the offset. During the determination of the offset only discharges that fell within the range of discharges previously measured and used in the building of the stage-discharge

relation were used in order to avoid extrapolation errors. If surveying data were available to relate pressure transducer location from year to year it was compared to the calculated offset for confirmation. Once the offset was determined, discharge measurements from the newest year were added to the stage-discharge relation to increase its accuracy and range. The cumulative stage-discharge relation was then used to convert the stage data into hydrographs, within this paper hydrographs created using the stage-discharge relations are referred to as gauged hydrographs.

4.2 Muskingum Routing

For each reach the gauged hydrograph at the upstream location was routed to the next gauging site downstream. The only exception is the northernmost reach of the Kuparuk River (Lower Kuparuk) located on the coastal plain. For this reach, the gauged hydrographs for site 2A and the Toolik River were added together and the resulting hydrograph was routed downstream to the USGS gauging site.

Hydrographs for each gauging site were routed downstream using the Muskingum method. Each reach was divided into a number of segments to satisfy the stability requirement in Equation 6, the number of segments varied between reaches as well as between years. The hydrographs were routed downstream one segment at a time using Equations 5-9, the output of one segment being used as the input for the next. For the determination of the values of K to be used, travel times were estimated for rain events with peak discharges that were discernable in both the upstream and downstream hydrographs. These travel times were then plotted as a function of the value of the upstream discharge associated with that individual peak. The points were then fit with a power curve to determine α and γ used in Equation 9. The upstream hydrograph was then routed and compared to the measured downstream hydrograph, at which point the values of α and γ were adjusted and the process repeated until the rising limbs and peaks of the routed hydrograph lined up with the downstream measured hydrograph.

The number of segments used in each reach was selected in order to be the minimum number of segments that still satisfied the second part of the stability requirement in Equation 6, $\Delta t \leq K$. A value of 0.25 was used for the attenuation coefficient X whenever possible. To satisfy the first part of the stability requirement, $2KX < \Delta t$, the value of the attenuation coefficient was reduced, resulting in a reduction of attenuation of the hydrograph. Reduction in the attenuation coefficient was generally only required during peaks in the hydrograph.

4.3 Routing Comparison

The error induced by this version of the Muskingum method was investigated through the comparison of the upstream gauged hydrograph and the routed hydrograph. The total discharge was calculated by integrating each hydrograph. The % increase in discharge due to routing was then calculated by subtracting the total discharge of the upstream gauged hydrograph from that of the routed hydrograph and dividing the result by the total discharge of the upstream gauged hydrograph.

The routed hydrographs determined using the Muskingum method were also compared to the routed hydrographs determined using a kinematic wave model, developed by Bethany Neilson and Tyler King of Utah State University for the instream temperature model, for the reaches from site 8 to site 7 and site 7 to site 5. To compare the hydrographs produced by the Muskingum method to those produced by the kinematic wave model the Nash-Sutcliffe Model Efficiency Coefficient (Krause et al., 2005) was calculated for each reach each year. For the Nash-Sutcliffe coefficient the closer the value is to 1 the more exact the match, where 1 represents an exact match and a value of 0 would result if a constant value of the mean were used.

4.4 Lateral Inflows and Runoff Ratios

The lateral inflow along each reach was determined by subtracting the routed upstream hydrograph from the downstream gauged hydrograph. For the Kuparuk River stilling well and Imnavait weir sites the lateral inflows were accepted as the gauged hydrograph as there were no upstream sites

that could be routed to their location. In order to compare the lateral inflows along the various reaches

the values were normalized by dividing by the contributing area for the reach. For each year the final

value at the end of each summer for the cumulative lateral inflow was divided by the final value of the

cumulative precipitation to calculate a runoff ratio for each reach.

There were some exceptions in the calculations for the reaches between the Kuparuk River

stilling well to site 5. For the reach from the Kuparuk River stilling well to site 8 the Imnavait confluence

gauged hydrograph was also subtracted from the site 8 gauged hydrograph in addition to the routed

hydrograph from the Kuparuk River stilling well. Due to a lack of high flow measurements at site 7 the

rating curve was insufficient to calculate high flow discharges, as a result the lateral inflows for the

reaches from site 8 to site 7 and site 7 and site 5 could not be determined individually. Flows were

instead routed downstream from site 8 to site 5 combining the two reaches into a singular larger reach.

4.5 Geospatial Measurements

The contributing area used in the determination of lateral inflows and in the construction of

precipitation records for each reach within the watershed was measured in ArcGIS. The Digital Elevation

Model (DEM) used during processing was built using two separate DEMs. A 5m resolution DEM that

covers the majority of the Kuparuk watershed (Nolan, 2003) was supplemented with a 25m resolution

DEM of the North Slope, Data Credit: National Elevation Dataset http://ned.usgs.gov/, both DEMs were

downloaded from http://toolik.alaska.edu/gis/data/ on September 15, 2014. The hydrology toolset

within the spatial analyst toolbox of ArcGIS was used to delineate the contributing area corresponding

to each gauging location. For each year a Thiessen polygon network was built for the available

meteorological stations using the proximity toolset within the analysis tools toolbox.

4.6 Precipitation

Available gauged precipitation datasets were examined for abnormalities and gaps in the record

before being accepted. Precipitation records for each reach were constructed based on the coverage of

the Thiessen polygons over the contributing area (Wurbs & James, 2002). The stations used and their

corresponding weights in building the precipitation record for each reach varied between 2013 and

2014, as seen in Appendix D, due to the addition and removal of monitoring stations to the network.

5. Results

5.1 Hydrograph Creation

To enable the merging of the 2013 and 2014 discharge measurements an offset was required to adjust the 2014 stage data to the 2013 datum, this was done using curve matching. The offsets determined using curve matching along with those determined using surveying data are shown in Table 5.1 for comparison, at the sites for which surveying data was available.

Table 5.1 Offsets for the adjustment of the 2014 stage data to the 2013 datum at sites for which surveying data were available for comparison against the curve matching method.

Site	Curve Matching (cm)	Surveying (cm)
Imnavait Confluence	-5.07	-2.71
Site 8	-0.82	-1.75
Site 7	-17.42	-16.89

The discharge measurements for both the 2013 and 2014 field seasons were plotted with respect to their final adjusted stage value and fit with a power curve of the form of Equation 10. Table 5.2 provides a summary of the constants Ω, η, and the R^2 value of the fitted curve for each site. The rating curve for each site is located in Appendix A.

Table 5.2 Constants for the stage-discharge relationship for each site and the corresponding R^2 value.

Site	Ω	η	R^2
Kuparuk River Stilling Well	2.662E-07	3.835	0.996
Imnavait Weir (Low Flow)	1.494E+03	4.556	0.864
Imnavait Weir (High Flow)	4.747E+02	2.919	0.937
Imnavait Confluence	4.612E+00	2.777	0.992
Site 8	2.396E-10	5.044	0.993
Site 7	3.195E-08	4.434	0.985
Site 5	5.735E-06	3.338	0.984
Site 4	1.191E-04	2.768	0.996
Site 3T	8.382E-04	2.254	0.996
Site 3B	1.352E-03	2.258	0.991
Site 2A	2.338E-06	3.510	0.998
Toolik River	4.286E-05	2.968	0.993

Equation 10 was then used with the corresponding constants from Table 5.1 to convert the stage record for both years at each site into continuous hydrographs. The hydrographs for each site, located in Appendix B, show the calculated discharge for each gauging site as well as when the calculated discharge exceeds the maximum measured discharge by more than 20% or drops below 80% of the minimum measured discharge.

5.2 Routing

The Muskingum method with variable travel time was used in order to route flows downstream from one gauging site to the next. The values of α and γ used in the determination of travel times, Equation 9, along with the minimum value of X that was used to satisfy the stability requirement, Equation 6, are shown in Table 5.3. Comparison between the upstream gauged hydrograph and the routed hydrograph revealed that the Muskingum method resulted in a slight increase in total discharge during routing, the percent increases in flow that occurred within each reach are shown in Table 5.3.

Table 5.3 Constants used for the calculation travel time for routing along with the minimum value of the attenuation coefficient, "X", and percent increase in flow within each reach due to routing for each year.

Reach	α	γ	2013		2014	
			Min "X"	% Increase in Flow	Min "X"	% Increase in Flow
Kuparuk River Stilling Well to Site 8	10.48	-0.692	0.043	0.83	0.067	0.56
Imnavait Weir to Imnavait Confluence	2.14	-0.940	0.110	9.68	0.085	6.42
Site 8 to Site 7	9.55	-0.663	0.064	0.67	0.083	0.50
Site 7 to Site 5	9.95	-0.388	0.065	0.94	0.114	0.84
Site 8 to Site 5	12.50	-0.414	0.110	0.81	0.152	1.31
Site 4 to Site 3T/3B	100.95	-0.382	0.099	7.69	0.161	2.17
Site 3T/3B to Site 2A	86.52	-0.375	0.214	2.19	0.210	0.37
Site 2A and 2T.1 to the USGS Gauge	68.83	-0.311	N/A		0.237	0.31

The routed hydrographs for the Muskingum method and the kinematic wave model for the reaches from site 8 to site 7, site 7 to site 5, and site 8 to site 5 are shown in Figure 5.1 for the 2013 field season and in Figure 5.2 for the 2014 field season. The routed hydrographs for the final rain event experienced in 2014 are shown in Figure 5.3.
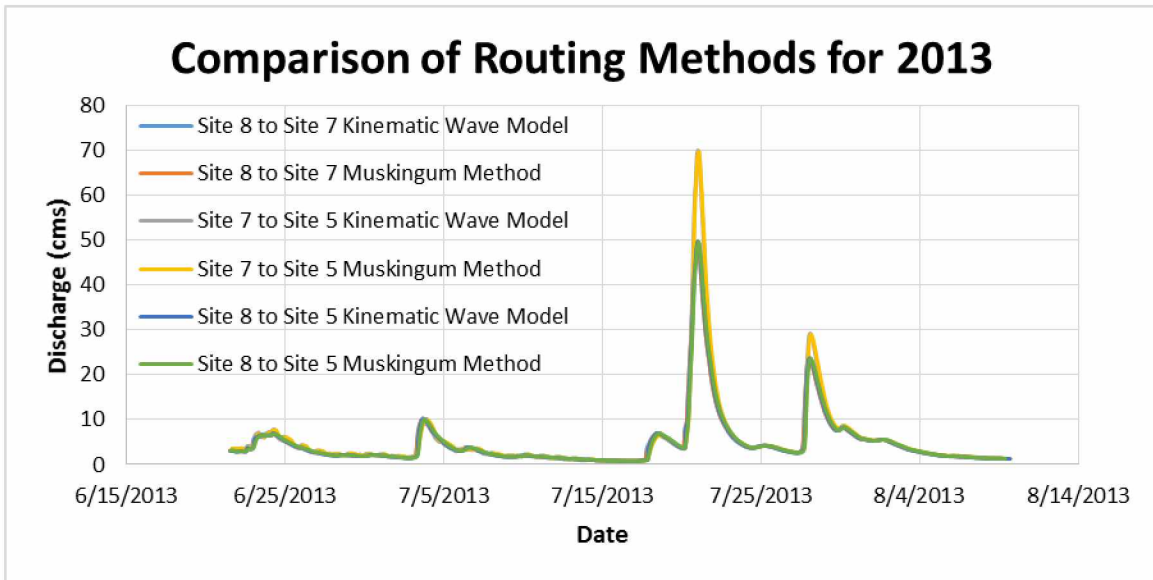
Figure 5.1 Comparison of the kinematic wave model to the Muskingum method for the reaches from site 8 to site 7, site 7 to site 5, and site 8 to site 5 in 2013.
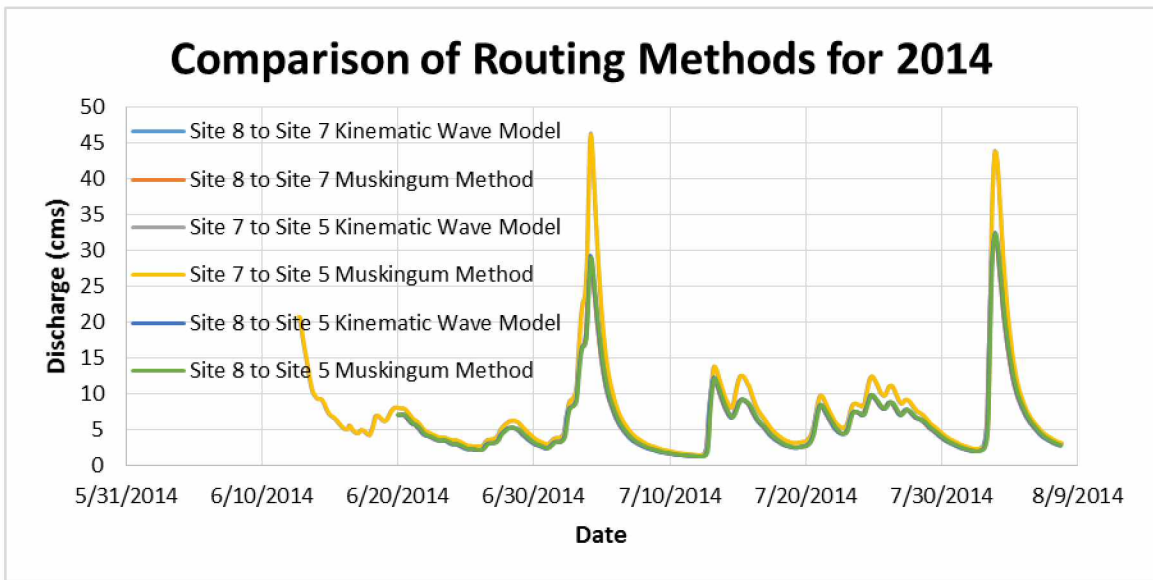
Figure 5.2 Comparison of the kinematic wave model to the Muskingum method for the reaches from site 8 to site 7, site 7 to site 5, and site 8 to site 5 in 2014.
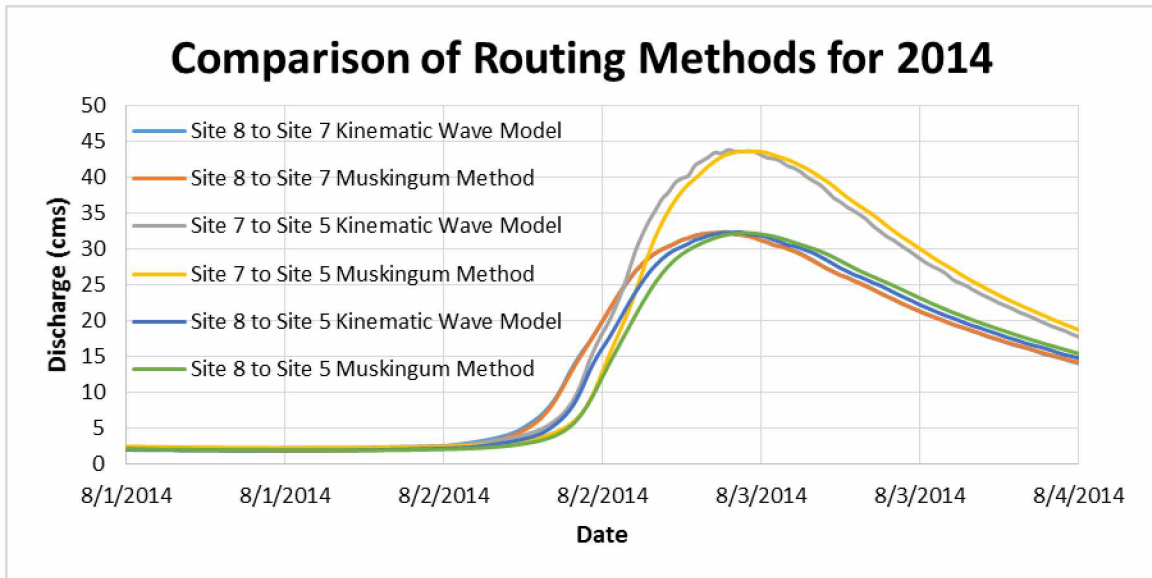
Figure 5.3 Comparison of the kinematic wave model to the Muskingum method for the reaches from site 8 to site 7, site 7 to site 5, and site 8 to site 5 for the final rain event of 2014.

The Nash-Sutcliffe Model Efficiency Coefficients comparing the routed hydrographs created using the Muskingum method to those of the kinematic wave model for each reach each year are shown in Table 5.4.

Table 5.4 Nash-Sutcliffe Model Efficiency Coefficients comparing the hydrographs routed using the Muskingum method to the hydrographs routed using the kinematic wave model.

Reach	Nash-Sutcliffe Model Efficiency Coefficient	
	2013	2014
Site 8 to Site 7	0.9996	0.9998
Site 7 to Site 5	0.9933	0.9930
Site 8 to Site 5	0.9948	0.9964

5.3 Lateral Inflows and Precipitation

The routed hydrographs produced using the Muskingum method were subtracted from the downstream gauged hydrographs to determine the lateral inflows. The cumulative lateral inflows were calculated throughout each summer and normalized by the contributing drainage area for each reach. The cumulative lateral inflows for each reach are shown for 2013 and 2014 collectively in Figure 5.4 and Figure 5.5, respectively, and individually in Appendix C. Maps showing the meteorological stations and

Thiessen polygon networks used to calculate the precipitation records are located in Appendix D, the

cumulative precipitation records were calculated over the same period of record for which the lateral

inflow data were available for each reach and are shown in Figure 5.6 for 2013 and Figure 5.7 for 2014.

The runoff ratios, calculated by dividing the cumulative later inflow by the cumulative

precipitation at the end of each summer, are shown in Table 5.5.
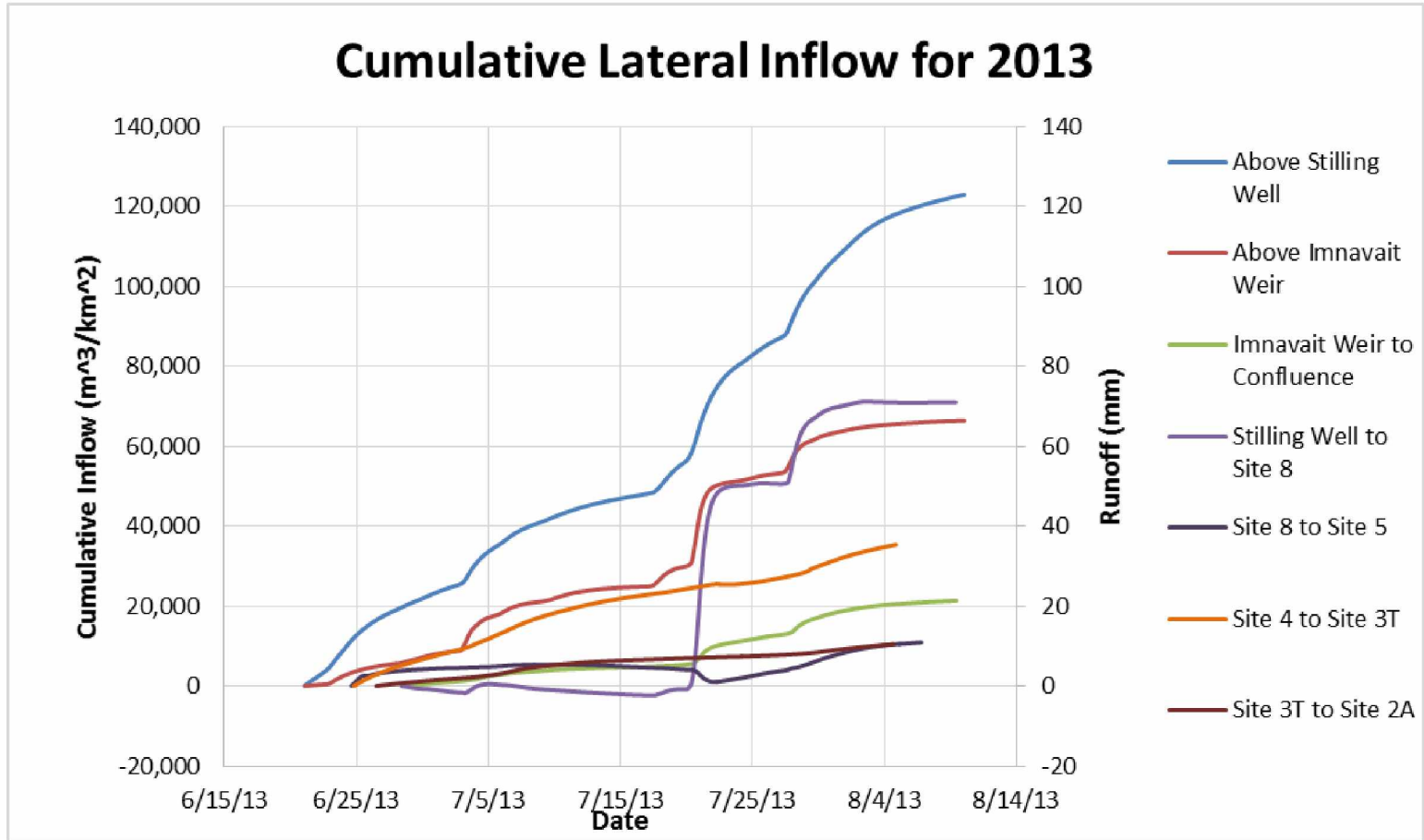
Figure 5.4 Cumulative lateral inflow for each reach during the 2013 field season.
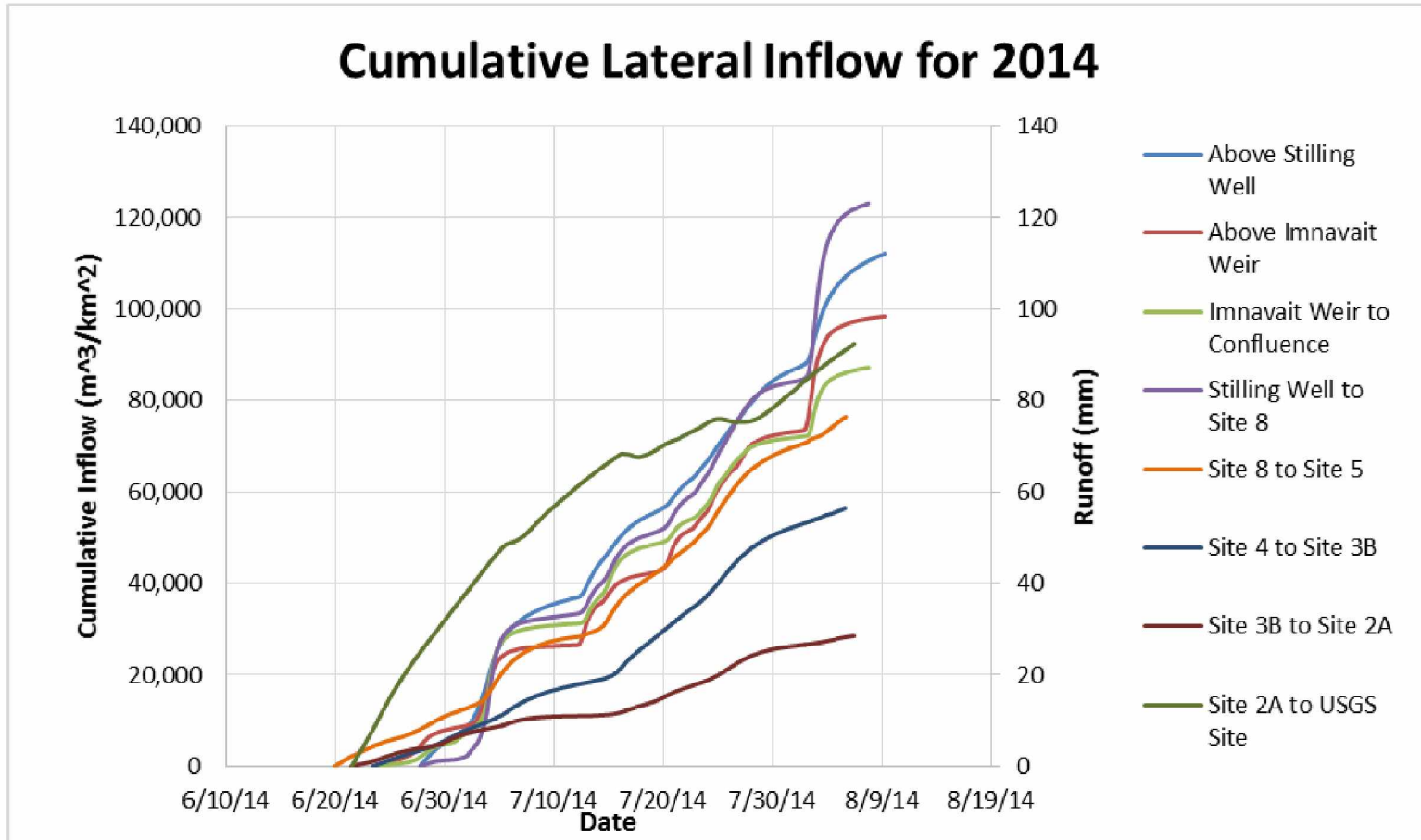
Figure 5.5 Cumulative lateral inflow for each reach during the 2014 field season.
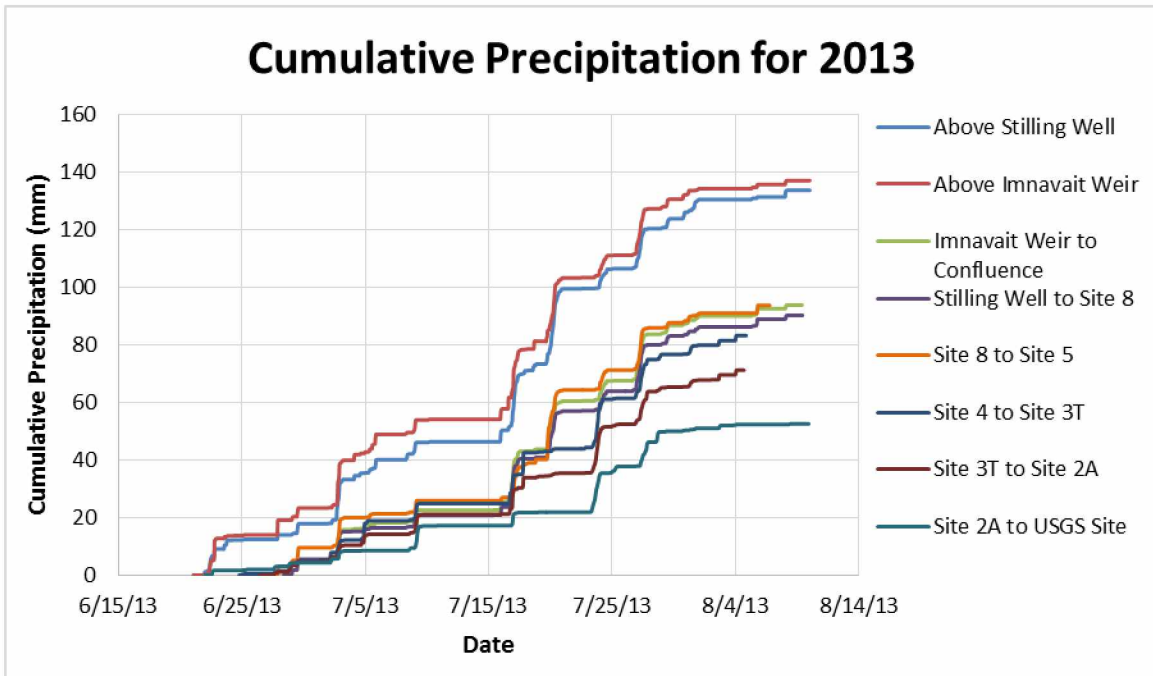
Figure 5.6 Cumulative precipitation for each reach during the 2013 field season.
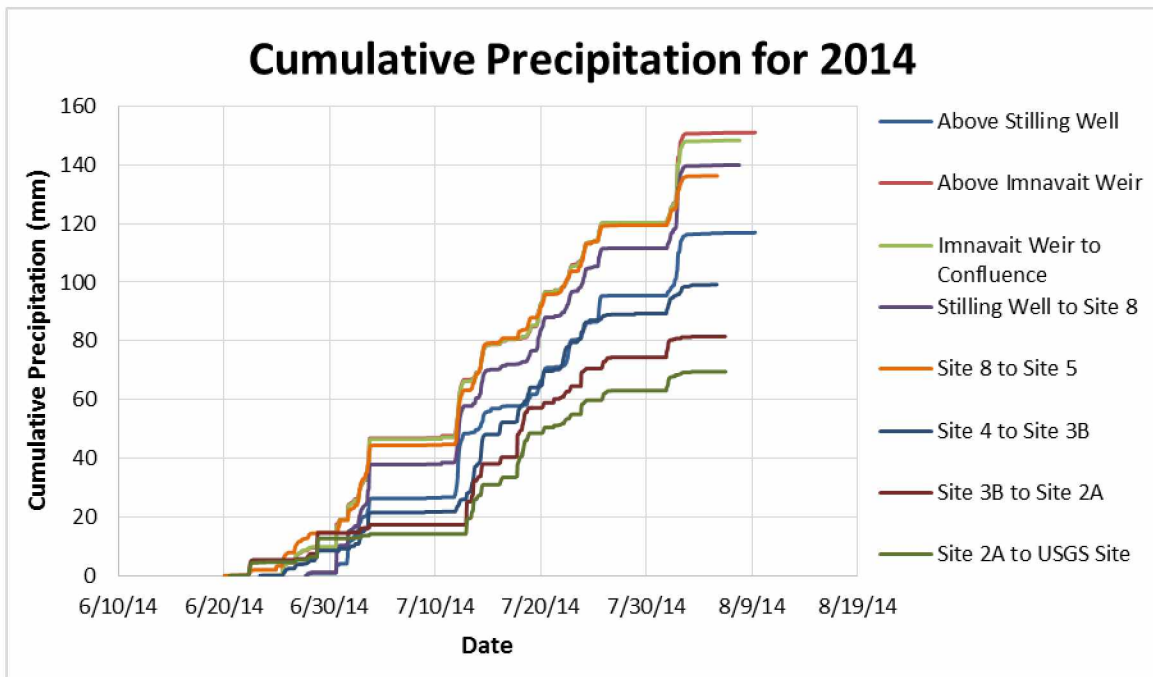
Figure 5.7 Cumulative precipitation for each reach during the 2014 field season.

Table 5.5 Runoff Ratios for each reach by year.

Reach	Runoff Ratio	
	2013	2014
Above the Kuparuk River Stilling Well	0.92	0.96
Above Imnavait Weir	0.48	0.65
Imnavait Weir to Confluence	0.23	0.59
Kuparuk River Stilling Well to Site 8	0.79	0.88
Site 8 to Site 5	0.12	0.56
Site 4 to Site 3T	0.42	N/A
Site 4 to Site 3B	N/A	0.57
Site 3T to Site 2A	0.15	N/A
Site 3B to Site 2A	N/A	0.35
Site 2A to USGS Site	N/A	1.33

6. Discussion

6.1 Hydrographs

The agreement between the two years of discharge measurements shown in Appendix A, the R^2 values in Table 5.2, and the agreement between the two methods of determination shown in Table 5.1 indicate that the year to year stage adjustment used was appropriate. Also, any morphological changes occurring within the channel between the two years did not alter the rating curve significantly. The R^2 values of Table 5.2 also attest to the suitability of the stage-discharge equations used to calculate the discharge while flows are within the measured range. Flows that exceed the measured range were estimated using the rating curve and are believed to exceed the actual flow within the channel, extension of the rating curve beyond the measured range requires the assumption that the channel geometry at higher flows was consistent with that of the channel geometry at lower flows during which the rating curve was developed. These estimates become less accurate as the stage continues to increase beyond the measured range, but serve as the best estimates currently available. These overestimates of the discharge result in overestimation of the lateral inflows and runoff ratio for the upstream reach, and an underestimation of the lateral inflows and runoff ratio of the downstream reach. The majority of flows throughout the two field seasons of record were within the maximum/minimum measured values, as shown in Appendix B.

Flows at the Toolik River site, site 2A, and site 3B exceeded the measured range repeatedly throughout the summer, more so than the other sites. This was due to the remote location of the sites and compounded by the fact that there was only one year of discharge measurements available to be used in the building of the stage-discharge relationships for the Toolik River site and site 3B. The discharges of site 8, site 7, and the Imnavait confluence site also exceeded the largest measured discharge, these occurrences were due to the flashy response of runoff to precipitation at these sites. The peaks at these sites were short in duration often making it difficult to arrive at the site while flows

were high, and occasionally upon arrival it was observed that the flows had increased to where it was no longer safe to enter the water and obtain a measurement. Although flows exceeded the measured range repeatedly throughout both field seasons the periods of exceedance were short in duration leaving the majority of the record unaffected and enabling the impacts to be isolated and traced.

The hydrographs for site 7 in Appendix B show that during peak flow events the extrapolated discharge exceeds the measured range by up to 7 times in 2013 and 4 times in 2014. The frequent occurrence and scale of exceedance resulted in the removal of site 7 and the merging of the reaches from site 8 to site 7 and site 7 to site 5 for the calculation of lateral inflows. We hope to erase this problem during the 2015 field season.

6.2 Routing

The Muskingum method was used with variable travel times to route flows from one gauging location downstream to the next. The minimum values of the attenuation coefficient "X" shown in Table 5.3 indicate that during peak flows attenuation of the routed hydrograph was reduced in order to satisfy the stability requirement. The values for the % increase in flow, shown in Table 5.3, indicate that the routing did not alter the total discharge from the routed hydrograph at the downstream end of the reach from that of the inflow hydrograph at the upstream end of the reach, except in the case of the reaches from the Imnavait weir to the Imnavait confluence and site 4 to site 3T. In these cases, the increase in total discharge due to routing would have the effect of underestimating the lateral inflows, and result in a reduced runoff ratio.

This Muskingum method was compared to the kinematic wave routing method, which will be used for the instream temperature model, for the reaches from site 8 to site 7, from site 7 to site 5, and site 8 to site 5 as these were the only reaches for which the kinematic wave model had been calibrated. It should be noted that although the kinematic wave method used a number of physical parameters, several of them were estimated and then adjusted to make the routed hydrographs match the

downstream measured hydrographs in a similar method to that of the calibration process used for the Muskingum method.

It can be seen in Figures 5.1-5.3 the hydrographs routed using the Muskingum method experienced a slight increase in the attenuation of the peaks and an overall greater amount of smoothing. The routed hydrographs from the two methods appeared very similar to one another, to determine the level of similarity for each pair of hydrographs, the Nash-Sutcliffe Model Efficiency Coefficient was calculated. The values shown in Table 5.1 (with a minimum value of 0.9930 for the six comparisons) indicate that the Muskingum method is a close approximation to the kinematic wave method, and is suitable for our purposes.

6.3 Lateral Inflows and Precipitation

The routed hydrographs were subtracted from the downstream hydrographs to determine the lateral inflows along each reach; the lateral inflows were then summed throughout the study period and these cumulative lateral inflows are shown in Figure 5.4 and Figure 5.5. The values for the cumulative precipitation of each sub watershed plotted in Figures 5.6 and 5.7 were consistent with previous studies (Kane et al., 2008; Kane et al., 2014) that showed summer precipitation increases moving away from the coast and into the foothills. The accuracy of the precipitation estimates became increasing problematic moving north within the watershed as the area attributed to each meteorological station increased. The total precipitation and total cumulative lateral inflow for each sub watershed were used to calculate the runoff ratios for the study period in Table 5.5.

Figures 5.4 and 5.5 show the general trend of progressively increasing values for the cumulative lateral inflows of reaches located farther south; similarly, subwatersheds located farther south, closer to the foothills, were determined to have higher values for the runoff ratio. Three reaches appear to be anomalies to both trends in 2013 (the Kuparuk River stilling well to site 8, the Imnavait weir to Imnavait

43

confluence, and site 8 to site 5) and one reach in 2014 (the confluence between the Toolik River and the Kuparuk River to the USGS gauging site).

Quantitative comparisons were attempted to investigate possible relationships between lateral inflows and watershed slope and shape. The results were inconclusive due to variations between watersheds in the duration, intensity, and cumulative amount of precipitation experienced leading up to, during, and after precipitation events. Comparisons were further stymied by the varying level of error introduced during the extrapolation of high flow discharge values between gauging sites.

For the majority of the 2013 field season the reach from the Kuparuk River Stilling well to site 8 was observed to lose water, positive lateral inflows (gains) to the reach were only experienced following precipitation events. The hydrograph for site 8 in 2013, located in Appendix B, shows a direct relation between the extrapolated discharge following a large rain event on the 19th and 20th of July and a dramatic gain in the cumulative lateral inflows for the reach, suggesting that the lateral inflows surrounding the event are inflated, which would also result in an over estimation of the runoff ratio for the reach. In 2013 the adjacent reach to the north, from site 8 to site 5, experienced minimal lateral inflows throughout the summer. The overestimation of discharge at site 8 following the aforementioned rain event resulted in a reduction in the cumulative lateral inflows for the reach from site 8 to site 5, and an underestimation of the runoff ratio. The water lost along the reach from the Kuparuk River stilling well to site 8 was not observed to reenter the river upstream of the Kuparuk aufeis, this in conjunction with the low lateral inflows and runoff ratio for the reach from site 8 to site 5 suggests that water from the Kuparuk River is entering into storage along these two reaches. This supports the existence of a talik which acts as the source of the water feeding the aufeis formation (Figure 2.2) along the Kuparuk River (Yoshikawa et al., 2007). The same behavior was not observed during the 2014 field season, this is believed to be due to the increase of precipitation experienced in these reaches (approximately 50% more) during the study period.

During 2013 the reach from the Imnavait weir to Imnavait confluence also experienced reduced lateral inflows and a lower than expected runoff ratio. However, this occurrence is not believed to be connected with the losing of water to the talik feeding the Kuparuk aufeis and it is currently unexplained.

The reach above the USGS gauging site experienced lateral inflows at a nearly constant rate, decreasing slightly as the summer progressed, but for the most part was unaffected by precipitation. The runoff coefficient calculated had a value greater than 1 indicating that more water was gained by the river within the reach than was supplied to the subwatershed through precipitation, suggesting that snowmelt runoff continues to contribute to the Kuparuk River well into the summer. This long runoff time for snowmelt and little to no response to summer precipitation events can be explained by the coupling of the very low natural hydraulic gradient of the area and the abundance of lakes, ponds and wetlands which are often poorly connected hydraulically and slow to drain after snowmelt.

The increasing value of the runoff coefficients observed in the reaches to the south indicates that increases in precipitation are not solely responsible for the increased lateral inflows. The increasing values of the runoff coefficients is believed to be due to a combination of steeper slopes within the southern watersheds, vegetation variability, and watershed shape.   Examination of the lateral inflow graphs, Appendix C, show that the reaches located farther to the south also experience larger contributions per square kilometer during low flow conditions than those located farther north.

7. Conclusion

The calculated offsets enabled the multiple years of stage data and discharge measurements to be collated. The composite stage-discharge relation for each site provides an adequate estimation of the discharge while the flows remained within the measured range, and the best available estimation of those outside the measured range.

The Muskingum method with variable coefficients used was a suitable method of the flow routing for the Kuparuk River on the North Slope of Alaska, and provided travel times and attenuations that approximates those of the kinematic wave model for the reaches of which comparison was available.

In moving north through the Kuparuk watershed from the foothills to coastal plain the cumulative lateral inflow contribution and low flow lateral inflow contribution to the river per square kilometer decreased, as did the runoff ratio as a general trend. These were caused by changes in the precipitation, hillslope gradient, vegetation, and watershed shape. There were three reaches that were exceptions to this trend: the reach from the Kuparuk River stilling well to site 8, the reach from site 8 to site 5, and the reach between the confluence of the Kuparuk River with Toolik River and the USGS gauging location.

Along the reach from the stilling well to site 8, the Kuparuk River was observed to lose water during the summer of 2013, during which the adjacent reach to the north, site 8 to site 5, also experienced minimal lateral inflows and a reduced runoff ratio. Although the river is situated atop continuous permafrost, it is hypothesized that this water recharges a large talik that acts as the source

of the water feeding the downstream aufeis field throughout the winter while the river is frozen

(Yoshikawa et al., 2007).

The coastal plain between the confluence of the Kuparuk River and the Toolik River and the USGS gauging location experienced a significantly higher lateral inflow contribution throughout the summer than the areas to the south, and the lateral inflow was for the most part independent of precipitation. It is hypothesized that this is due to snowmelt stored in the low gradient topography composed of an abundance of slow draining lakes, ponds and wetlands. This conclusion is supported by prior research in the Putuligayuk watershed (Bowling et al., 2003).

8. Future work

This research would be further improved with the collection of additional years of field data. One more year of data collection is currently scheduled for the summer of 2015. Discharge measurements should be targeted such that high flow conditions are captured to increase the range of the stage-discharge relations. The new stage-discharge relations should then be used to recalculating the flows at each site for the 2013 and 2014 seasons as well as calculate the flows for the 2015 season. All flows should then be routed down river and the lateral inflows calculated; these lateral inflows should then be compared with special attention paid to the reaches from the Kuparuk River stilling well to site 8, site 8 to site 5 (if site 7 is still unusable), and from the confluence of the Kuparuk River with the Toolik River to the USGS gauging site for consistency with the previous years.

The determined lateral inflows will be used as inputs to calibrate the surface water temperature model. Once the model is calibrated it will be used to run possible climate change scenarios.

The Kuparuk River should be investigated from the Kuparuk River stilling well to the aufeis field to determine the nature of the talik that exists. It would be beneficial to the understanding of the hydrologic processes of the area to know the locations of connectivity between the talik and the river as well as the storage capacity of the talik and the residency time of the water within it.

References

Bedient, P. B., W. C. Huber and B. E. Vieux (2013). Hydrology and Floodplain Analysis. Prentice Hall.

Betts, E. D. and D. L. Kane (2015 In Press). "Linking North Slope Climate, Hydrology, and Fish Migration." *Hydrology Research.*

Bowling, L. C., D. L. Kane, R. E. Gieck, L. D. Hinzman and D. P. Lettenmaier (2003). "The Role of Surface Storage in a Low-Gradient Arctic Watershed." *Water Resources Research* 39(4): 1087-1099.

Cooter, E. J. and W. S. Cooter (1990). "Impacts of Greenhouse Warming on Water Temperature and Water Quality in the Southern United States." *Climate Research* 1(1): 1-12.

Cunge, J. A. (1969). "On the Subject of a Flood Propagation Computation Method (Musklngum Method)." *Journal of Hydraulic Research* 7(2): 205-230.

Gill, M. A. (1978). "Flood Routing by the Muskingum Method." *Journal of Hydrology* 36(3–4): 353-363.

Guang-Te, W. and V. P. Singh (1992). "Muskingum Method with Variable Parameters for Flood Routing in Channels." *Journal of Hydrology* 134(1–4): 57-76.

Hinzman, L., N. Bettez, W. R. Bolton, F. S. Chapin, M. Dyurgerov, C. Fastie, B. Griffith, R. Hollister, A. Hope, H. Huntington, A. Jensen, G. Jia, T. Jorgenson, D. Kane, D. Klein, G. Kofinas, A. Lynch, A. Lloyd, A. D. McGuire, F. Nelson, W. Oechel, T. Osterkamp, C. Racine, V. Romanovsky, R. Stone, D. Stow, M. Sturm, C. Tweedie, G. Vourlitis, M. Walker, D. Walker, P. Webber, J. Welker, K. Winker and K. Yoshikawa (2005). "Evidence and Implications of Recent Climate Change in Northern Alaska and Other Arctic Regions." *Climatic Change* 72(3): 251-298.

Hinzman, L., D. Kane and K. Everett (1993). "Hillslope Hydrology in an Arctic Setting". *Proceedings, Sixth International Conference on Permafrost*, South China Press Beijing, China, 257-271.

Hinzman, L. D., D. L. Kane, R. E. Gieck and K. R. Everett (1991). "Hydrologic and Thermal Properties of the Active Layer in the Alaskan Arctic." *Cold Regions Science and Technology* 19(2): 95-110.

Houghton, J. T., Y. Ding, D. J. Griggs, M. Noguer, P. J. van der Linden, X. Dai, K. Maskell and C. Johnson (2001). Climate Change 2001: The Scientific Basis. Cambridge University Press Cambridge.

Kane, D. L., L. Hinzman, C. Benson and K. Everett (1989). "Hydrology of Imnavait Creek, an Arctic Watershed." *Holarctic Ecology* 12(3): 262-269.

Kane, D. L., L. Hinzman, R. Gieck, J. McNamara, E. Youcha and J. Oatley (2008). "Contrasting Extreme Runoff Events in Areas of Continuous Permafrost, Arctic Alaska." *Hydrology Research* 39(4): 287-298.

Kane, D. L. and C. W. Slaughter (1972). "Seasonal Regime and Hydrological Significance of Stream Icings in Central Alaska." *Proceedings, the role of snow and ice in hydrology, Banff. International Association of Scientific Hydrology Publication*(107): 528-540.

Kane, D. L., K. Yoshikawa and J. P. McNamara (2013). "Regional Groundwater Flow in an Area Mapped as Continuous Permafrost, Ne Alaska (USA)." *Hydrogeology Journal* 21(1): 41-52.

Kane, D. L., E. K. Youcha, S. L. Stuefer, G. Myerchin-Tape, E. Lamb, J. W. Homan, R. E. Gieck, W. E. Schnabel and H. Toniolo (2014). "Hydrology and Meteorology of the Central Alaskan Arctic: Data Collection and Analysis. Final Report". University of Alaska Fairbanks, Water and Environmental Research Center, Report INE/WERC 14.05, Fairbanks, Alaska.

Krause, P., D. P. Boyle and F. Bäse (2005). "Comparison of Different Efficiency Criteria for Hydrological Model Assessment." *Adv. Geosci.* 5: 89-97.

Lawler, E. (1964). "Flood Routing." *US Army Corps of Engineers (ed.) Handbook of Applied Hydrology, Section*: 35-58.

Lilly, E. K., D. L. Kane, L. D. Hinzman and R. E. Gieck (2000). "Annual Water Balance for Three Nested Watersheds on the North Slope of Alaska". *Proceedings, Permafrost- Seventh International Conference*, Yelowknife, Northwest Territories, Centre d'études nordiques, Université Laval, 669-674.

Linsley JR., R. K., M. A. Kohler and J. L. H. Paulhus (1975). Hydrology for Engineers. 2nd Edition. New York, McGraw-Hill.

McNamara, J. P., D. L. Kane and L. D. Hinzman (1998). "An Analysis of Streamflow Hydrology in the Kuparuk River Basin, Arctic Alaska: A Nested Watershed Approach." *Journal of Hydrology* 206(1): 39-57.

Nolan, M. (2003). Distribution of a Star3i DEM of the Kuparuk River Watershed. Boulder, CO, Joint Office for Scientific Support.

Osterkamp, T. E. and M. W. Payne (1981). "Estimates of Permafrost Thickness from Well Logs in Northern Alaska." *Cold Regions Science and Technology* 5(1): 13-27.

Peterson, B. J., R. M. Holmes, J. W. McClelland, C. J. Vörösmarty, R. B. Lammers, A. I. Shiklomanov, I. A. Shiklomanov and S. Rahmstorf (2002). "Increasing River Discharge to the Arctic Ocean." *Science* 298(5601): 2171-2173.

Turnipseed, D. P. and V. B. Sauer (2010). Discharge Measurements at Gaging Stations. US Department of the Interior, US Geological Survey.

van Vliet, M. T. H., W. H. P. Franssen, J. R. Yearsley, F. Ludwig, I. Haddeland, D. P. Lettenmaier and P. Kabat (2013). "Global River Discharge and Water Temperature under Climate Change." *Global Environmental Change* 23(2): 450-464.

Walker, M. D., D. A. Walker and K. R. Everett (1989). "Wetland Soils and Vegetation, Arctic Foothills, Alaska". U.S. Department of the Interior Fish and Wildlife Service. 89(7), Fort Collins, CO.

Wood, C. M. and D. G. McDonald (1997). Global Warming: Implications for Freshwater and Marine Fish. Cambridge University Press.

Wurbs, R. A. and W. P. James (2002). Water Resources Engineering. Prentice Hall Upper Saddle River, NJ.

Yang, D., B. E. Goodison, S. Ishida and C. S. Benson (1998). "Adjustment of Daily Precipitation Data at 10 Climate Stations in Alaska: Application of World Meteorological Organization Intercomparison Results." *Water Resources Research* 34(2): 241-256.

Yoshikawa, K., L. D. Hinzman and D. L. Kane (2007). "Spring and Aufeis (Icing) Hydrology in Brooks Range, Alaska." *Journal of Geophysical Research: Biogeosciences* 112(G4): G04S43.

Appendix A: Rating curves used to convert stage values to discharge values
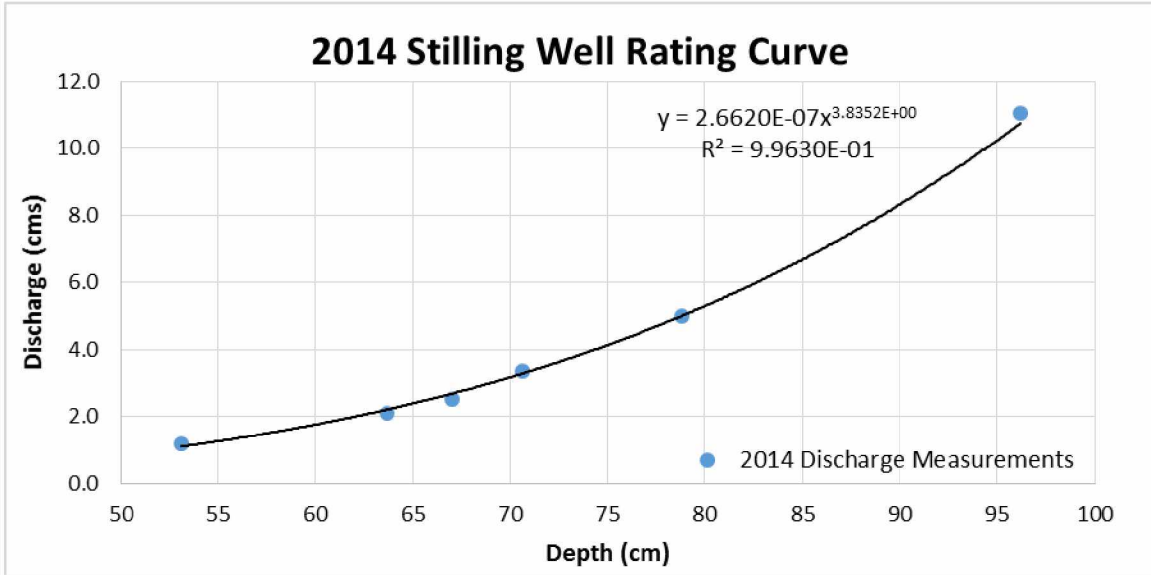
Figure A.1: Rating curve for the Kuparuk River stilling well.
Rating curve used to convert stage values to discharge values at the Kuparuk River stilling well site in 2014.
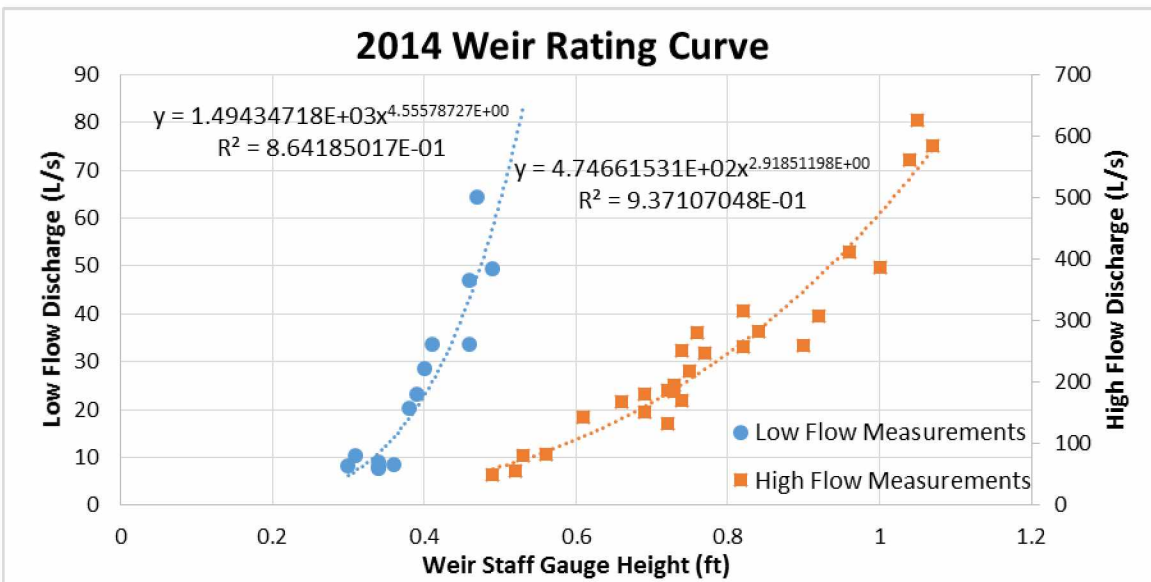
Figure A.2: Rating Curve for the Imnavait Creek Weir.
Rating Curve used to convert stage values to discharge values at the Imnavait Creek weir site in 2014, the low flow stage-discharge relation was used for stages under 0.49 ft.
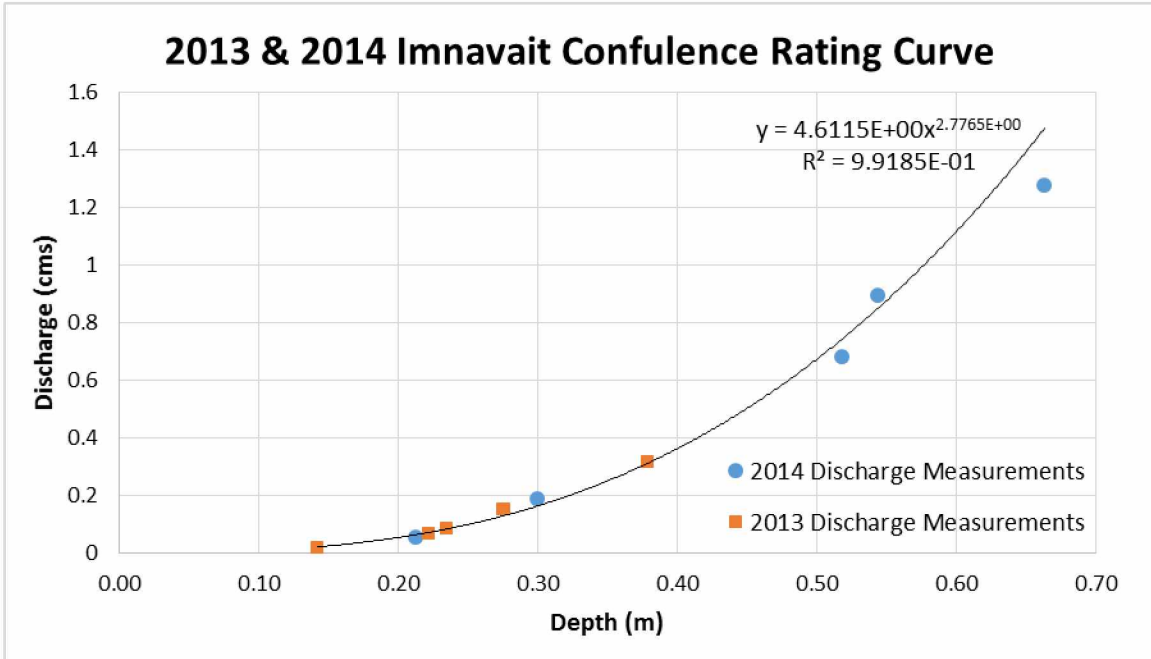
Figure A.3: Rating curve for the Imnavait Creek confluence.
Rating curve used to convert stage values to discharge values at the Imnavait Creek confluence site in 2013 and 2014.
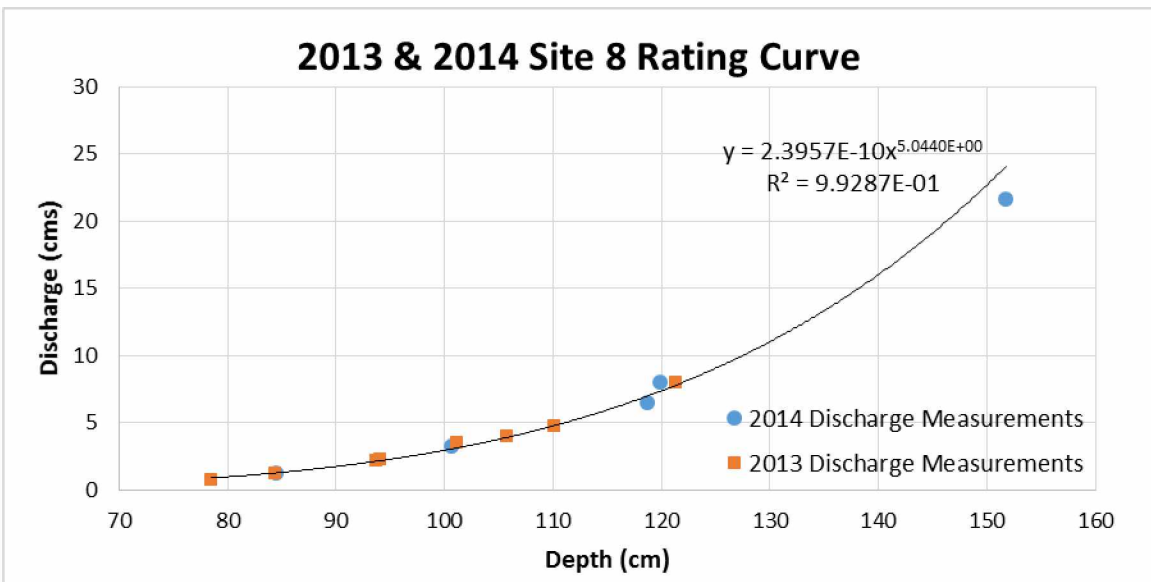
Figure A.4: Rating curve for site 8.
Rating curve used to convert stage values to discharge values at site 8 in 2013 and 2014.
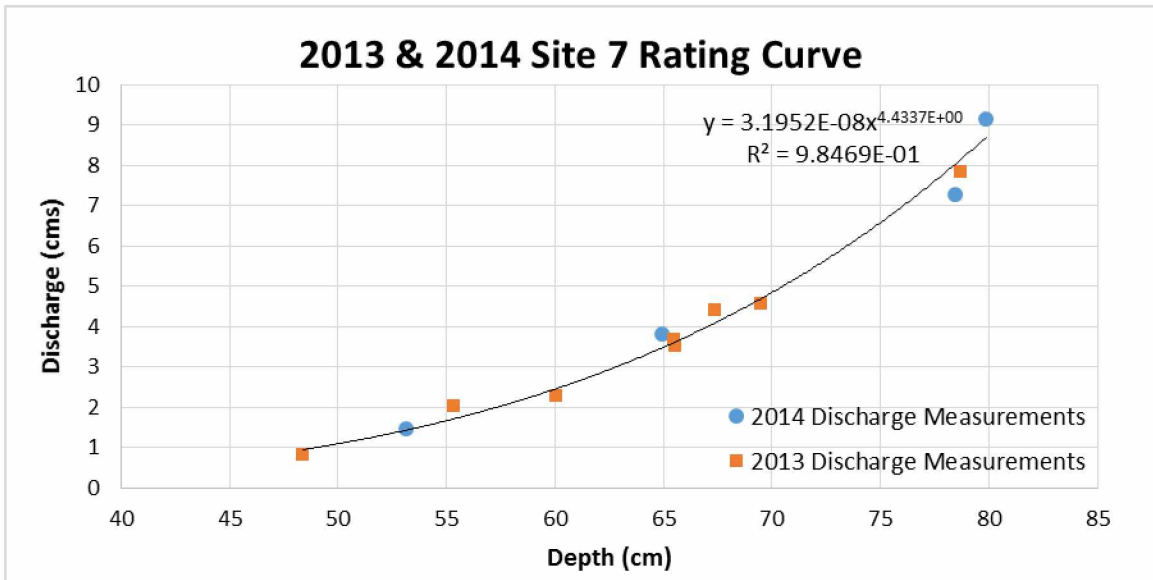
Figure A.5: Rating curve for site 7.
Rating curve used to convert stage values to discharge values at site 7 in 2013 and 2014.
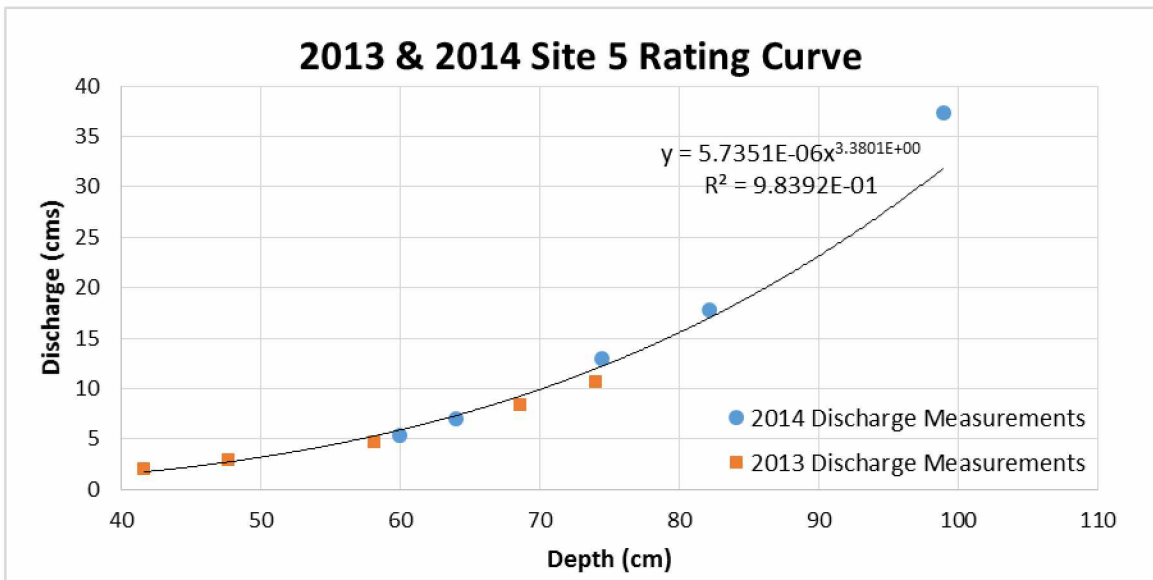
Figure A.6: Rating curve for site 5.
Rating curve used to convert stage values to discharge values at site 5 in 2013 and 2014.
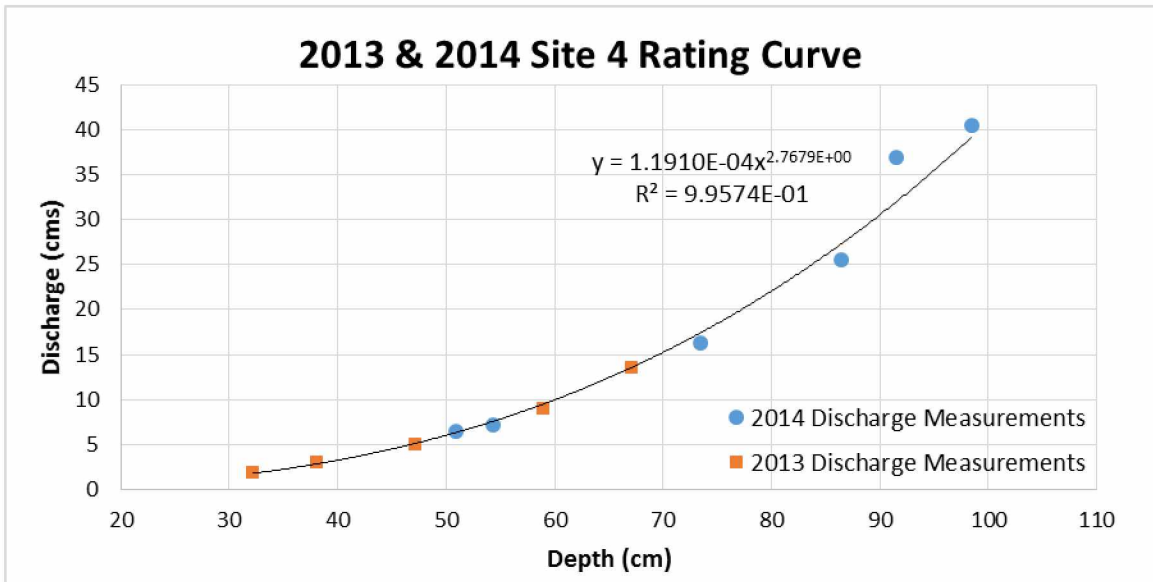
Figure A.7: Rating curve for site 4.
   Rating curve used to convert stage values to discharge values at site 4 in 2013 and 2014.
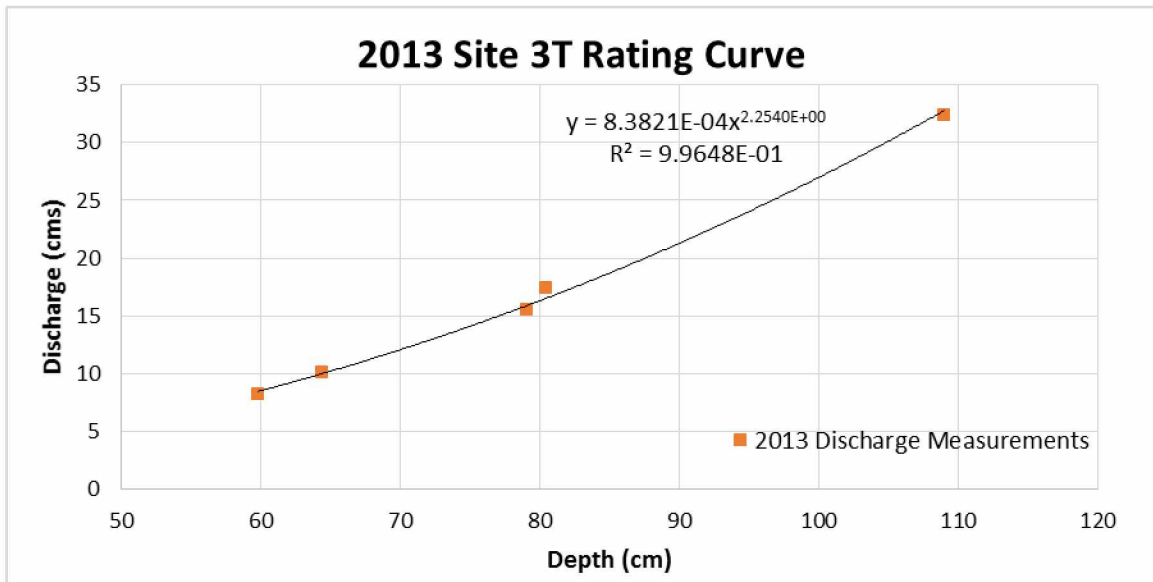
Figure A.8: Rating curve for site 3T.
   Rating curve used to convert stage values to discharge values at site 3T, above the White Hills River confluence, in 2013.
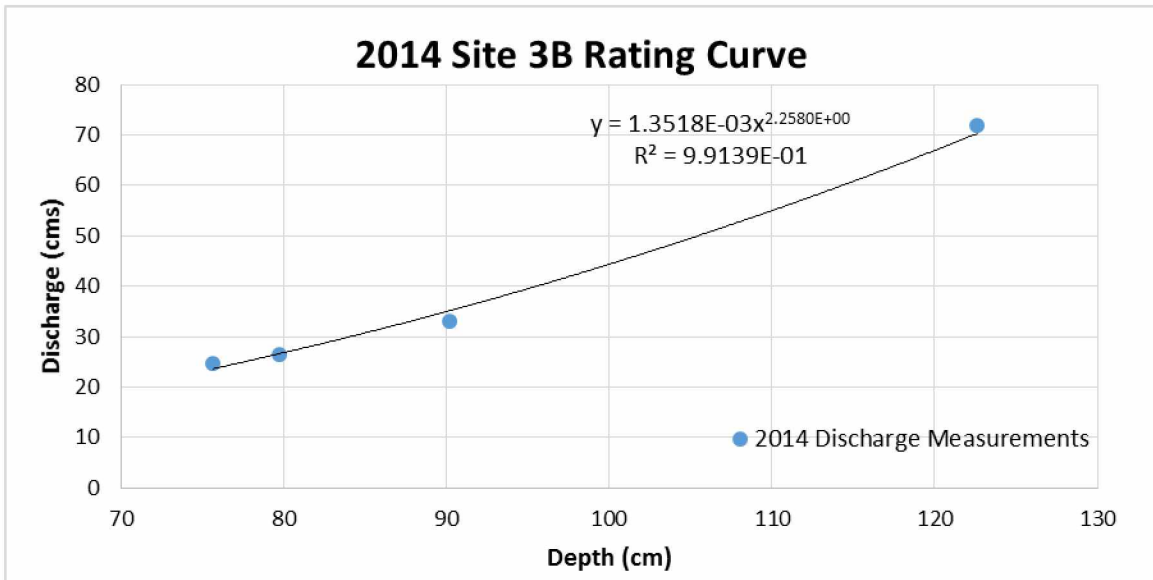
Figure A.9: Rating curve for site 3B

Rating curve used to convert stage values to discharge values at site 3B, below the White Hills River confluence, in 2014.
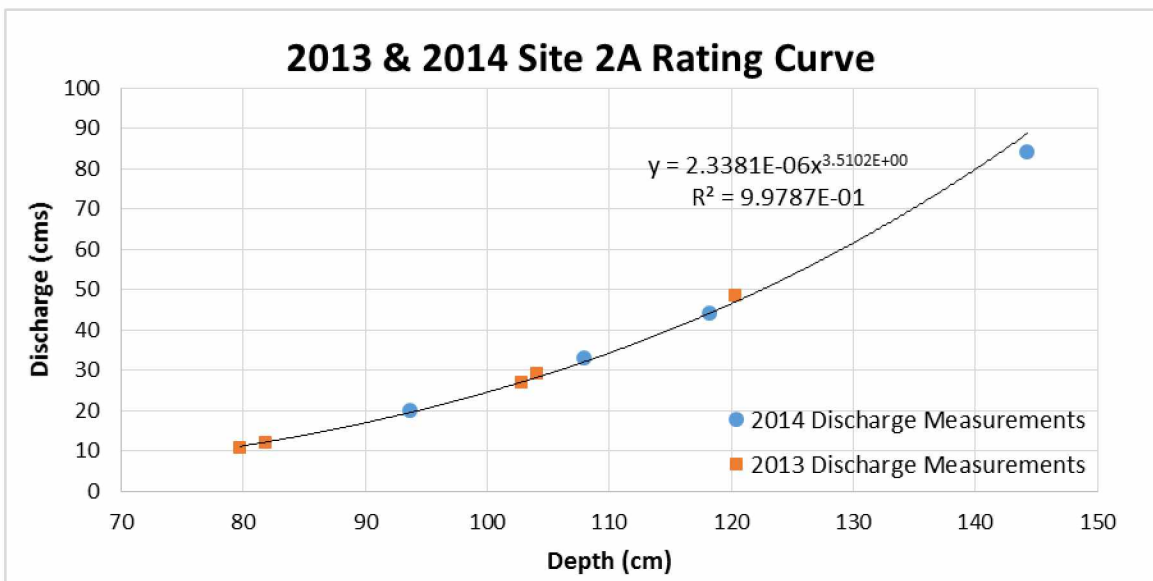
Figure A.10: Rating curve for site 2A.

Rating curve used to convert stage values to discharge values at site 2A, above the Toolik River confluence, in 2013 and 2014.
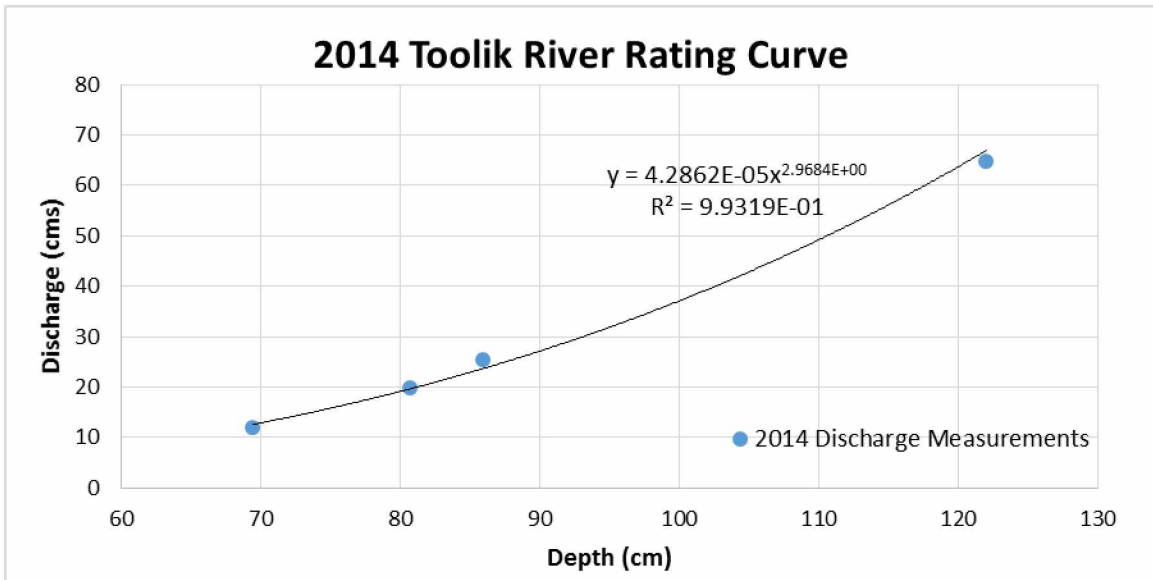
Figure A.11: Rating curve for the Toolik River.

Rating curve used to convert stage values to discharge values at the Toolik River site in 2014.

Appendix B

Appendix B: Gauged hydrographs for each year at each site

Extrapolated discharge values reflect values that are at least 20% outside of measured values.
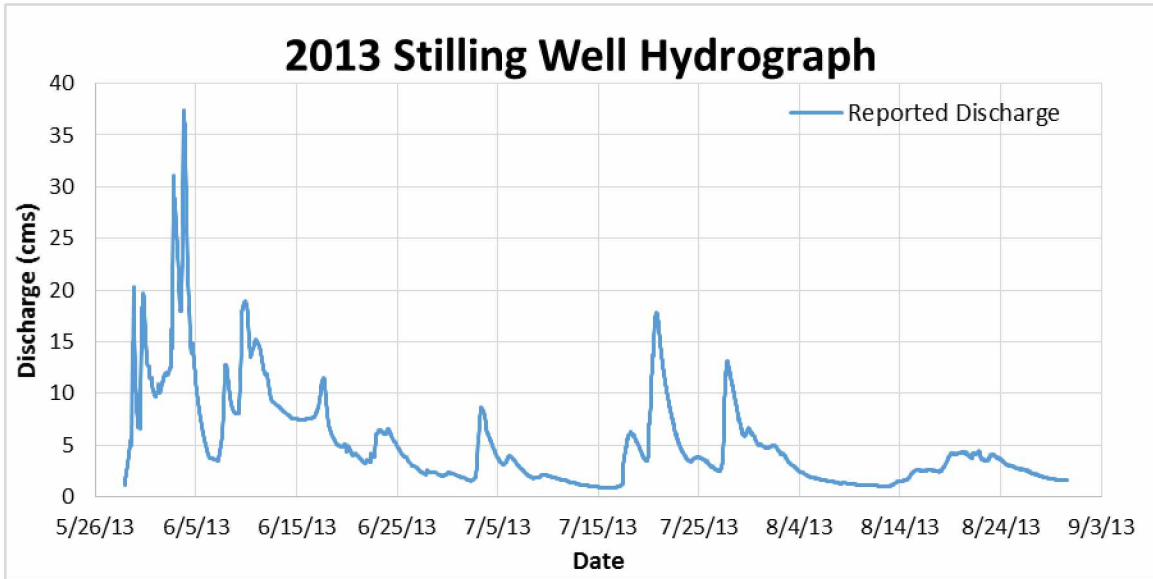
Figure B.1: Hydrograph for the Kuparuk River Stilling well in 2013.
        Hydrograph for the Kuparuk River stilling well in 2013 as reported by the WERC.
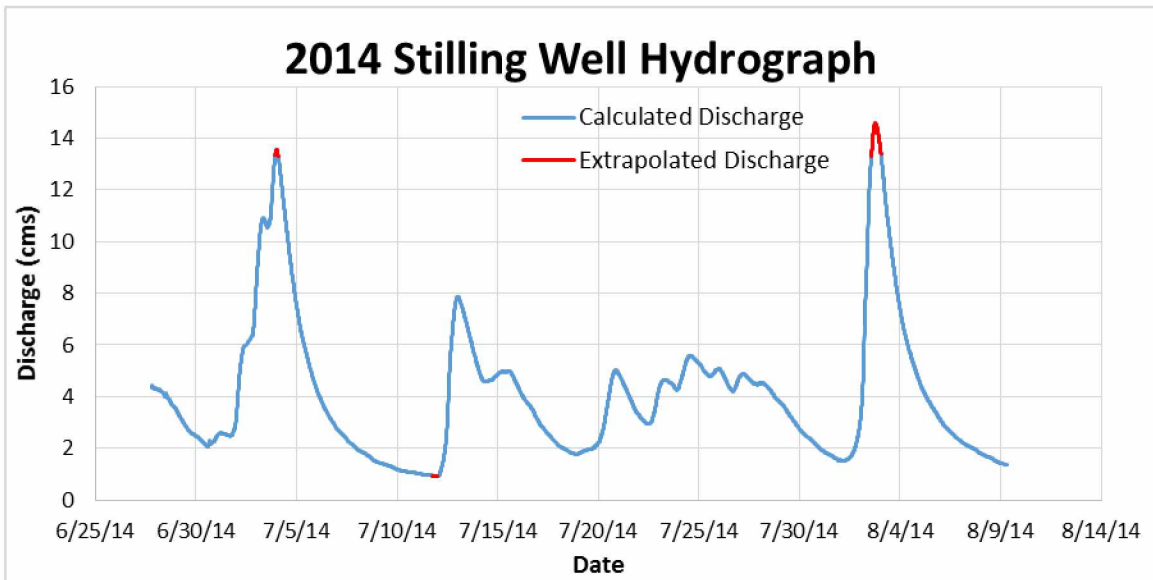
Figure B.2: Hydrograph for the Kuparuk River stilling well in 2014.
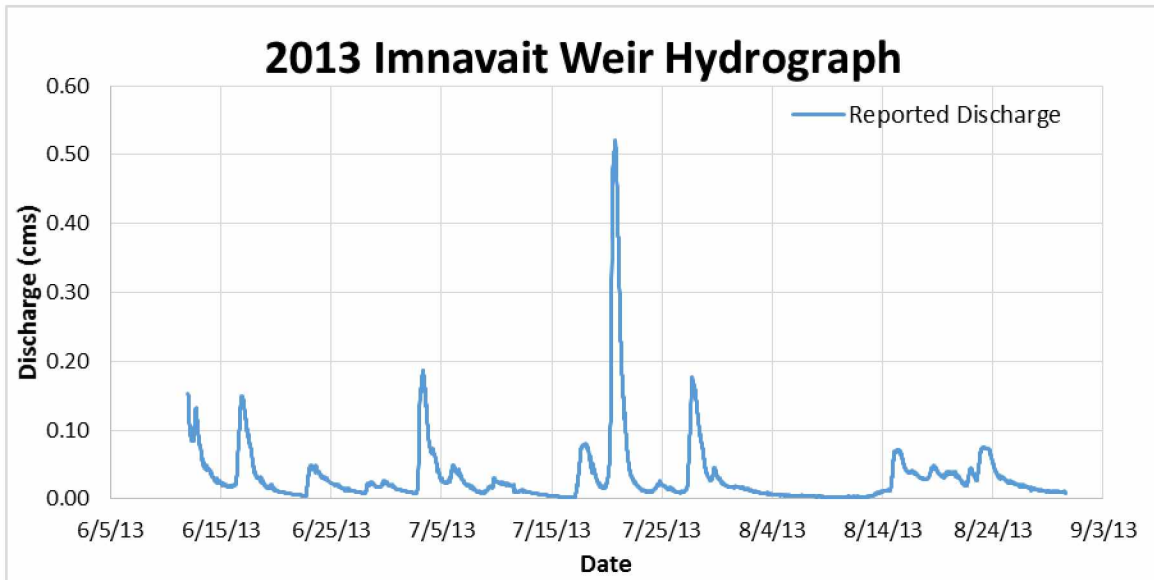
Figure B.3: Hydrograph for the Imnavait Creek weir in 2013.
Hydrograph for the Imnavait Creek weir in 2013 as reported by the WERC.
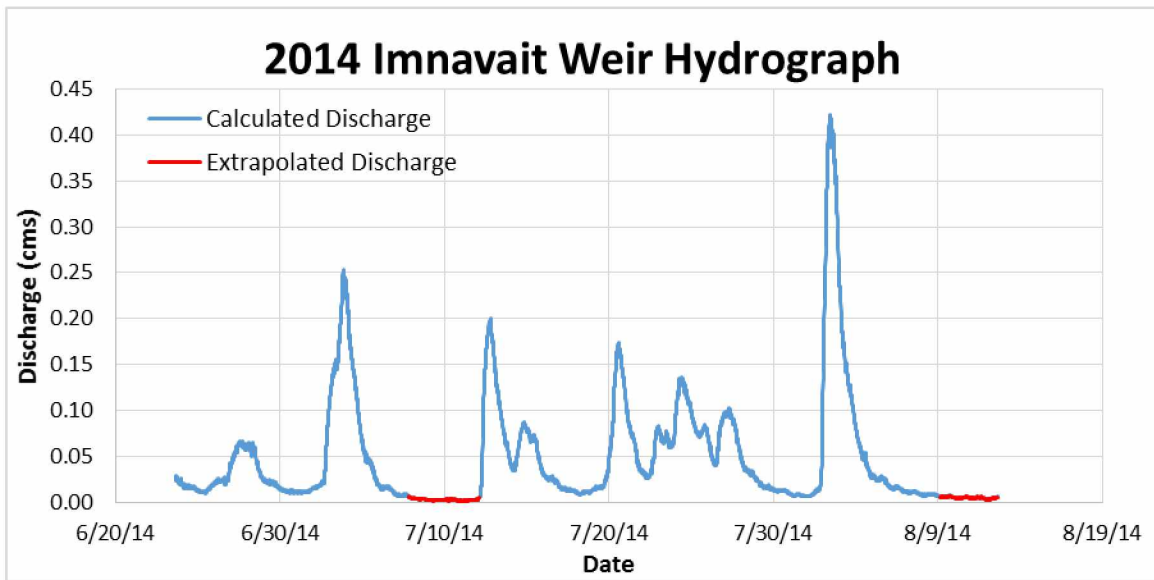
Figure B.4: Hydrograph for the Imnavait Creek weir in 2014.
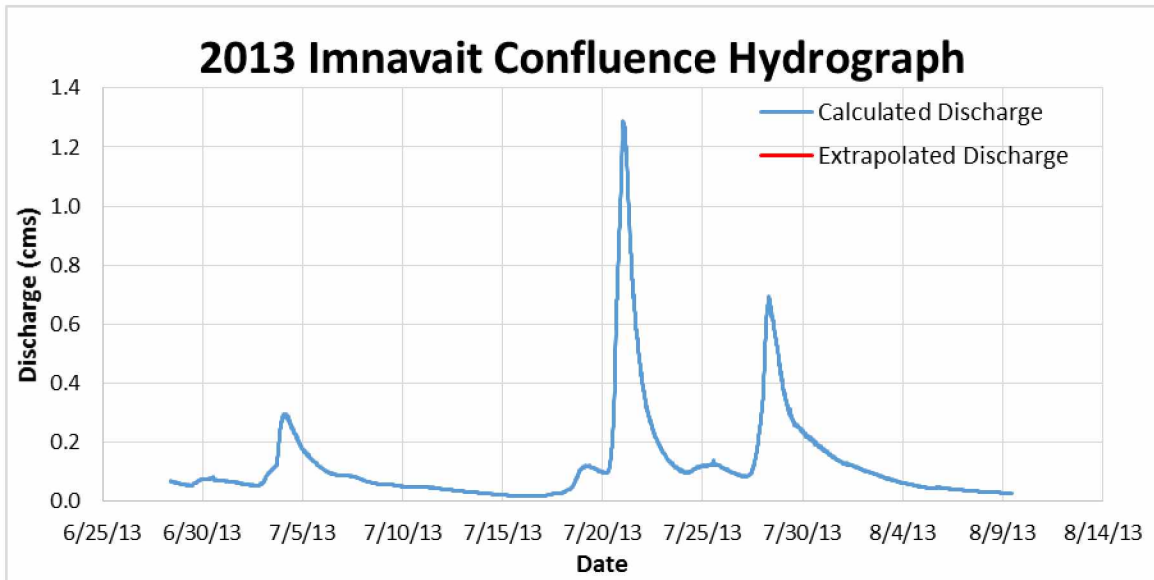
Figure B.5: Hydrograph for the Imnavait Creek confluence site in 2013.
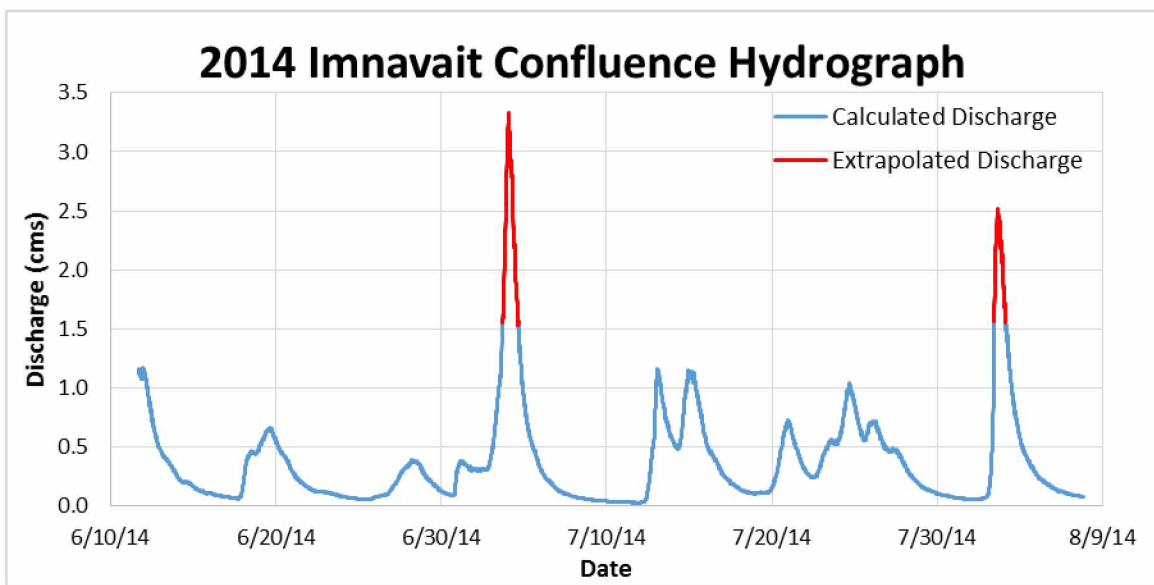
Figure B.6: Hydrograph for the Imnavait Creek confluence site in 2014.
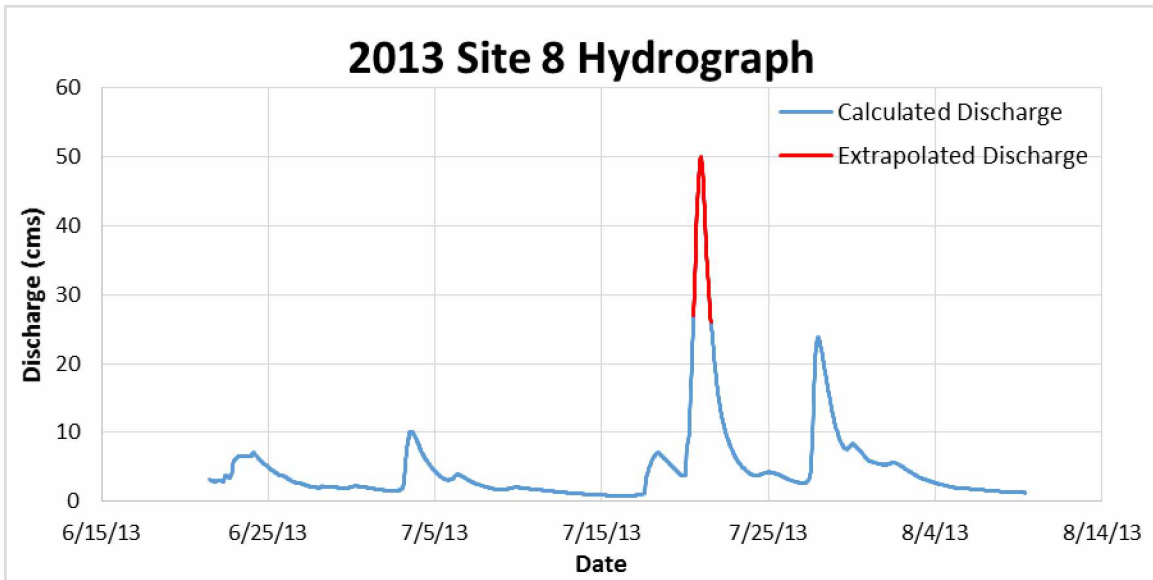
Figure B.7: Hydrograph for site 8 in 2013.
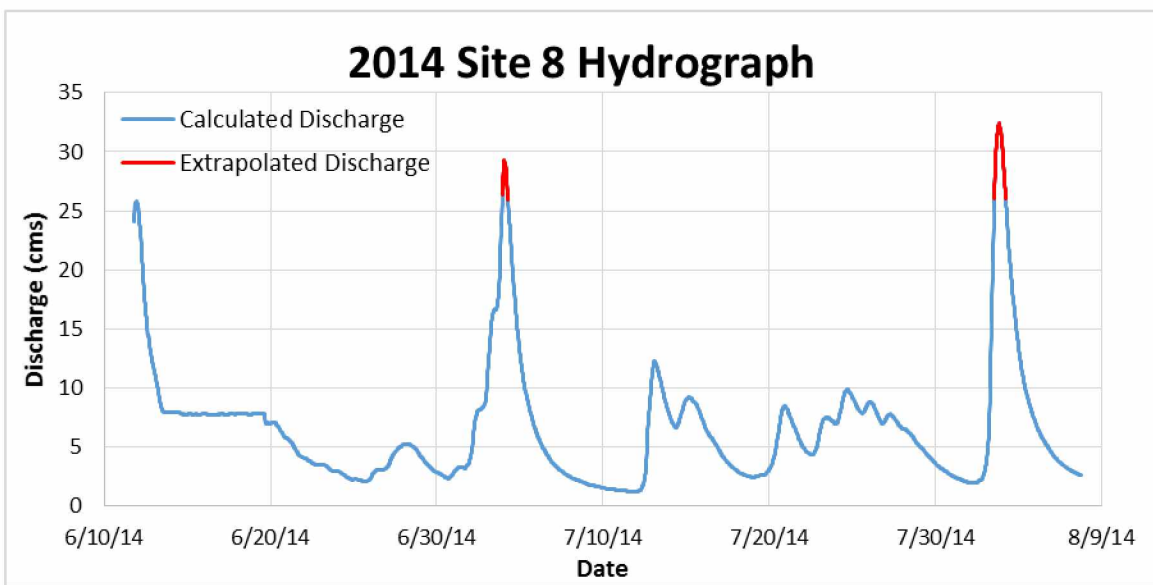
Figure B.8: Hydrograph for site 8 in 2014.
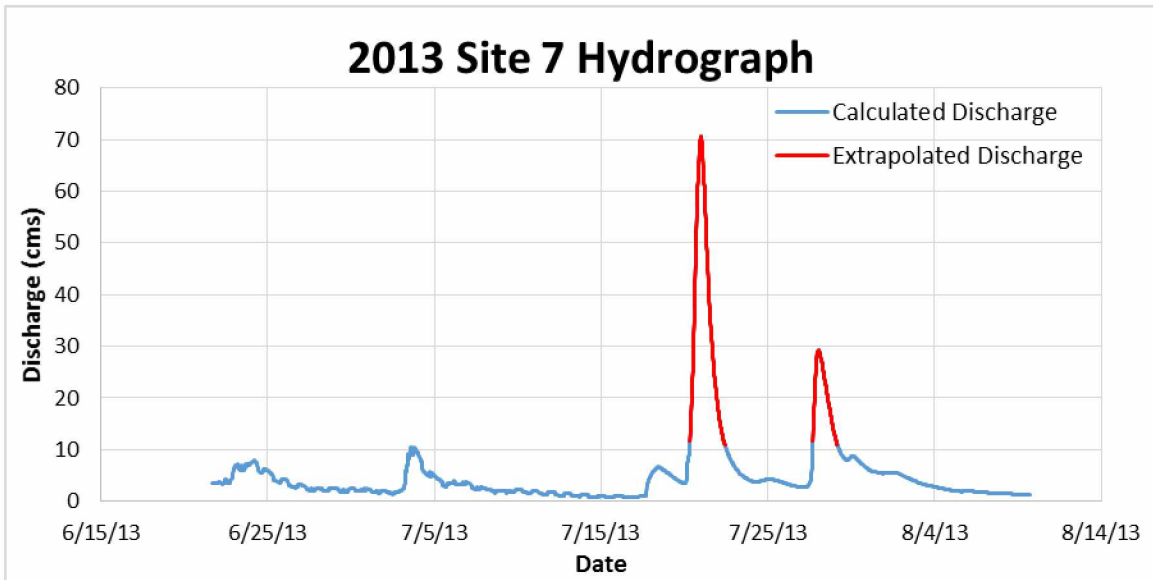
Figure B.9: Hydrograph for site 7 in 2013.
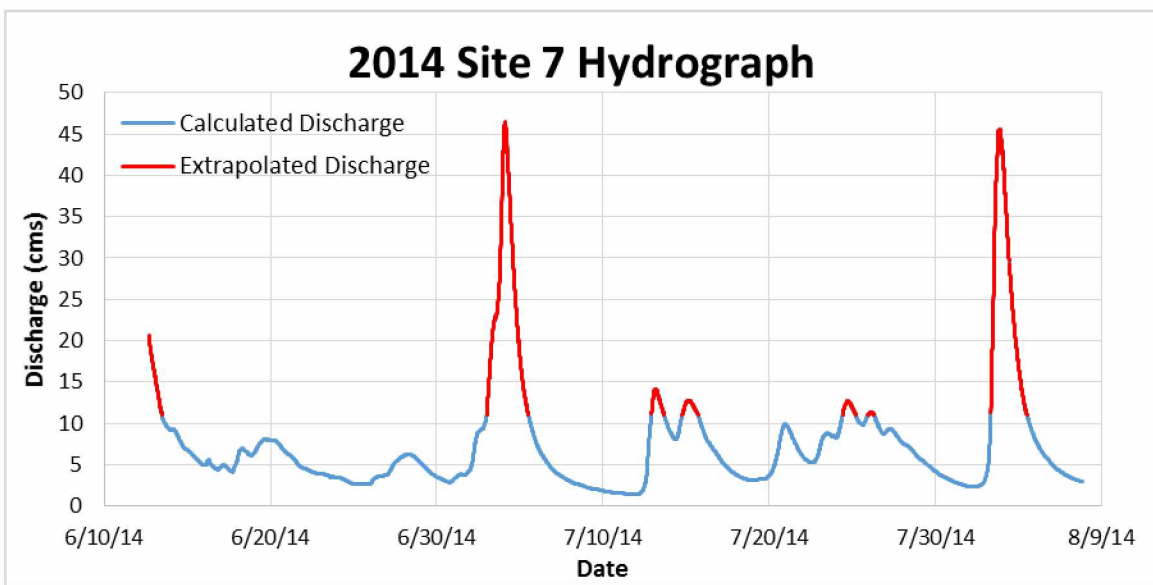
Figure B.10: Hydrograph for site 7 in 2014.
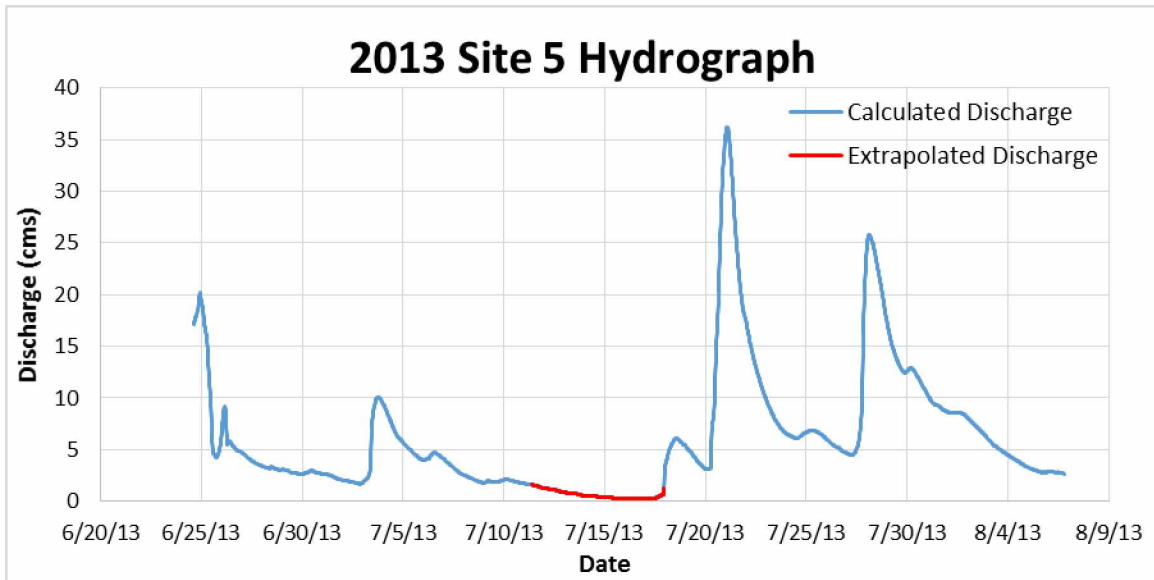
Figure B.11: Hydrograph for site 5 in 2013.
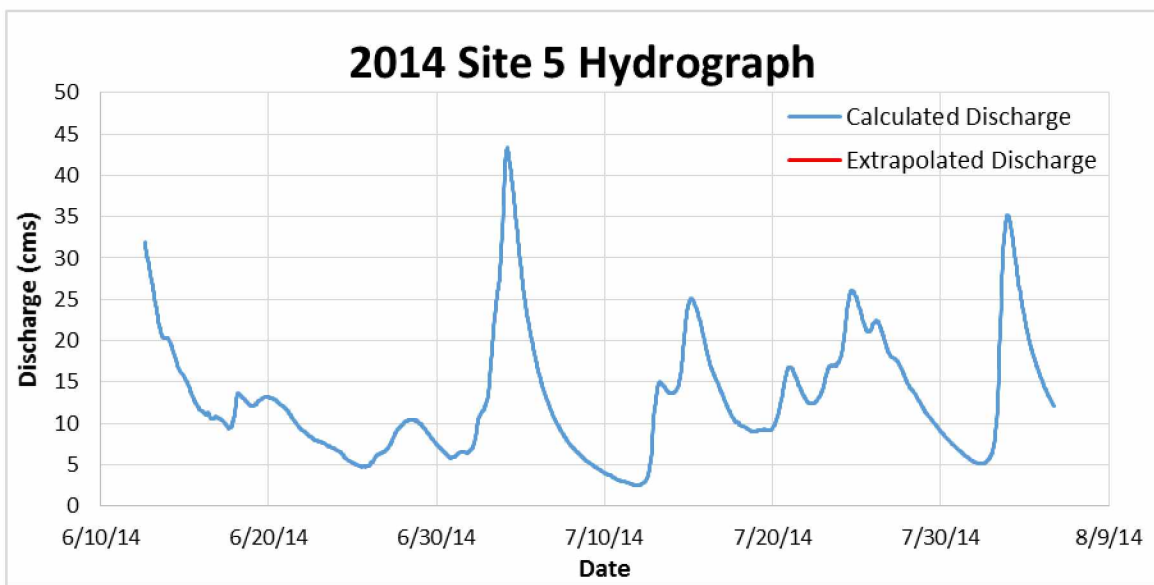
Figure B.12: Hydrograph for site 5 in 2014.
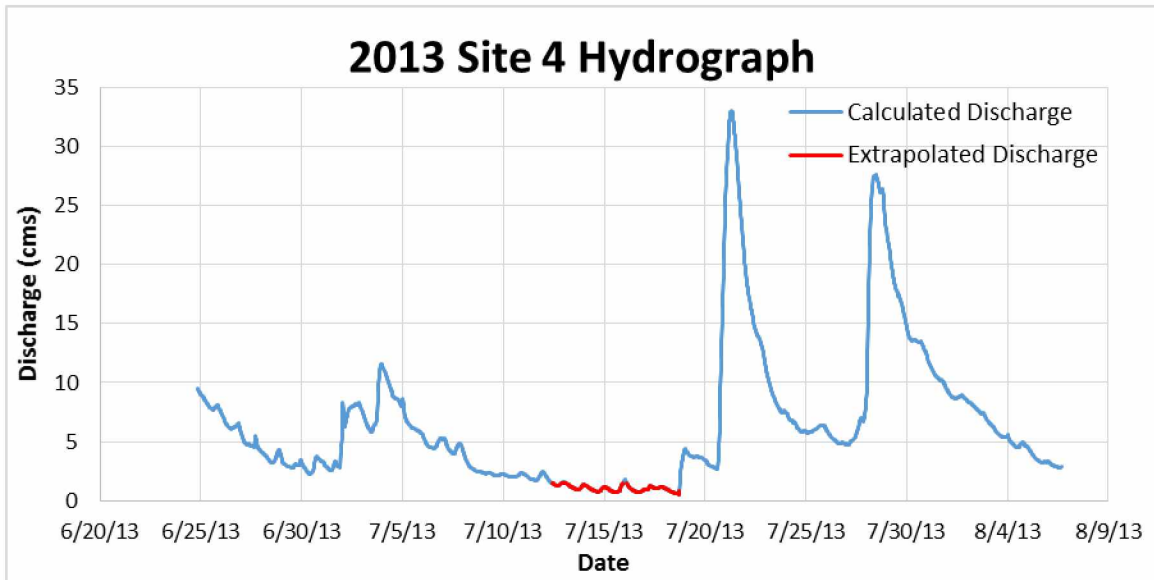
Figure B.13: Hydrograph for site 4 in 2013.
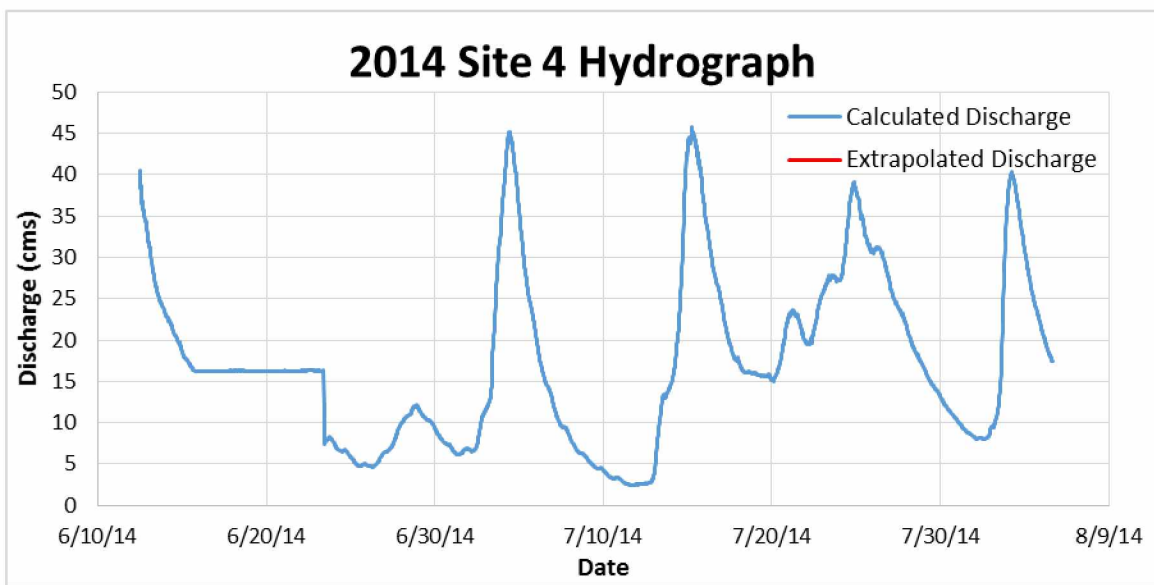
Figure B.14: Hydrograph for site 4 in 2014.
Hydrograph for site 4 in 2014, the sensor was out of the water from 6/15 to 6/23.
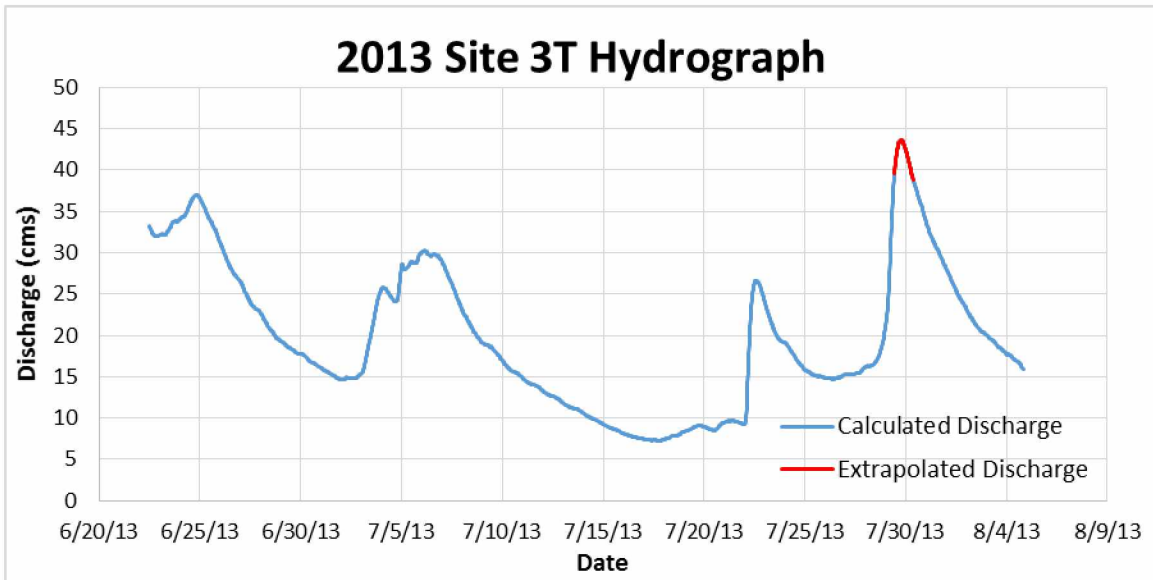
Figure B.15: Hydrograph for site 3T in 2013.
    Hydrograph for site 3T, above the White Hills River confluence, in 2013.
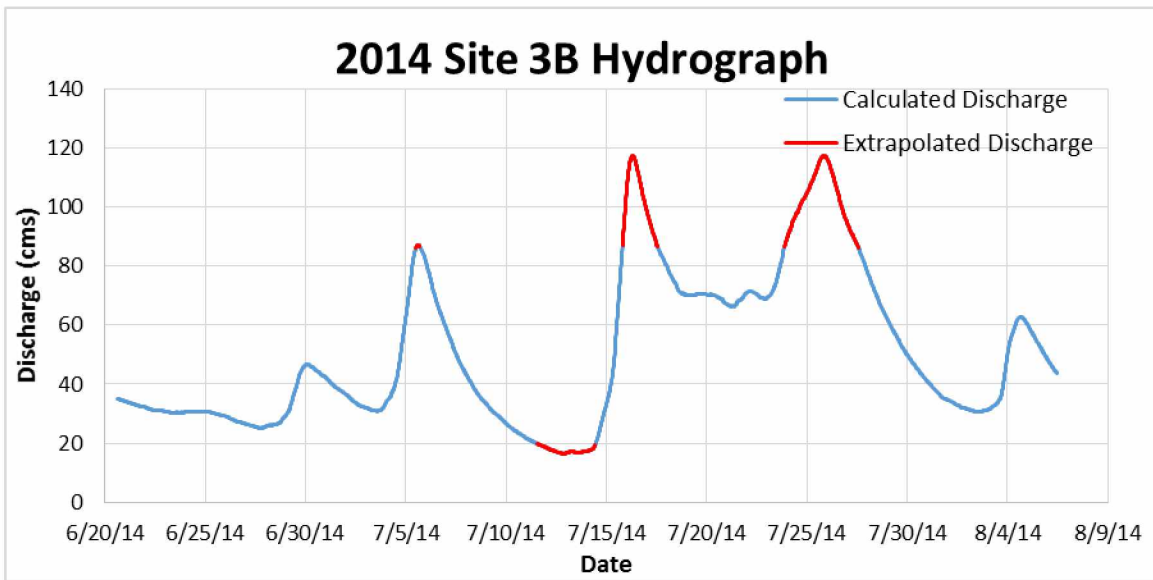
Figure B.16: Hydrograph for site 3B in 2014.
    Hydrograph for site 3B, below the White Hills River confluence, in 2014.
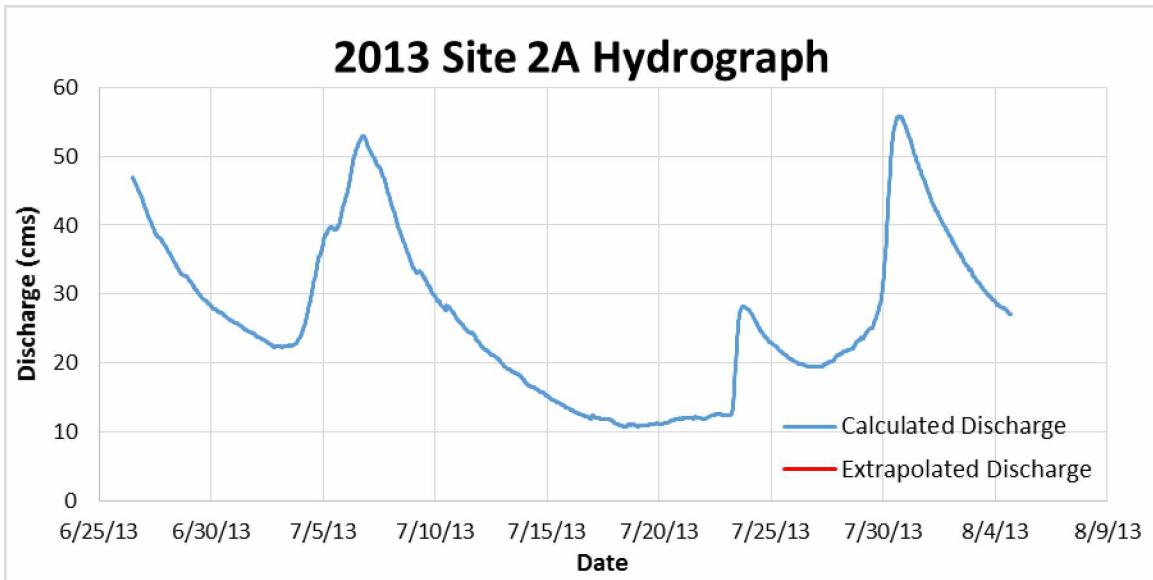
Figure B.17: Hydrograph for site 2A in 2013.
    Hydrograph for site 2A, above the Toolik River confluence, in 2013.
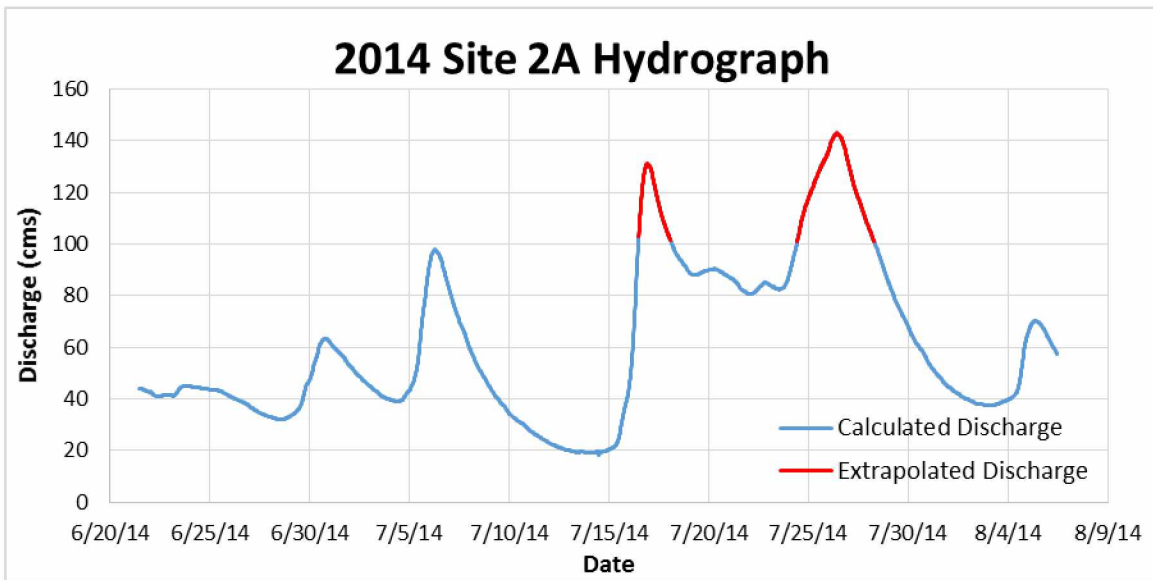
Figure B.18: Hydrograph for site 2A in 2014.
    Hydrograph for site 2A, above the Toolik River confluence, in 2014.
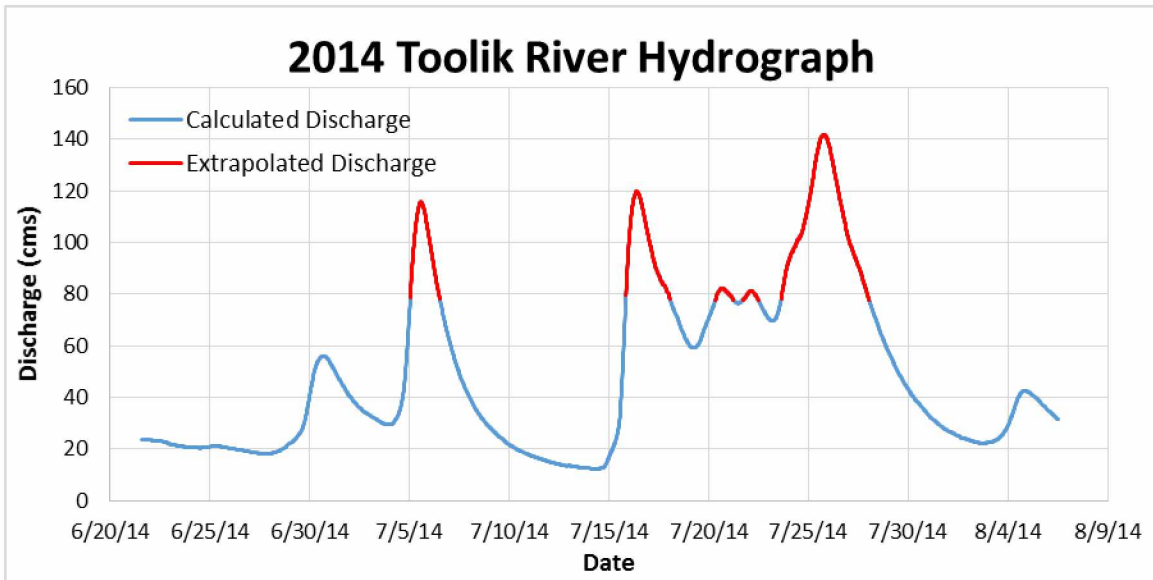
Figure B.19: Hydrograph for the Toolik River site in 2014.
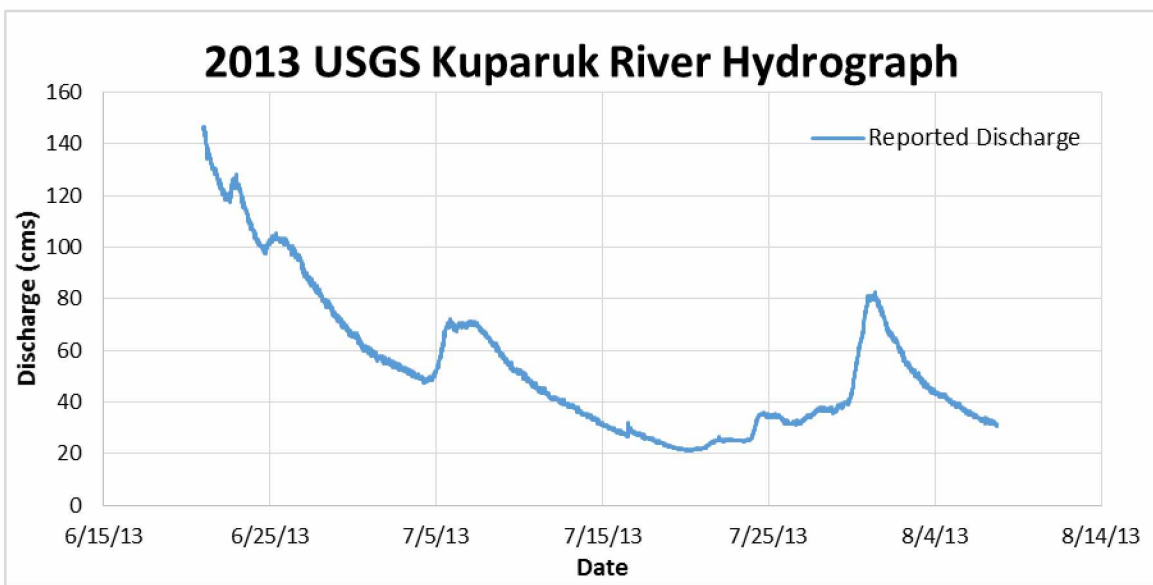
Figure B.20: Hydrograph for the USGS site in 2013.
Hydrograph for the USGS Kuparuk River site as reported by the USGS in 2013.
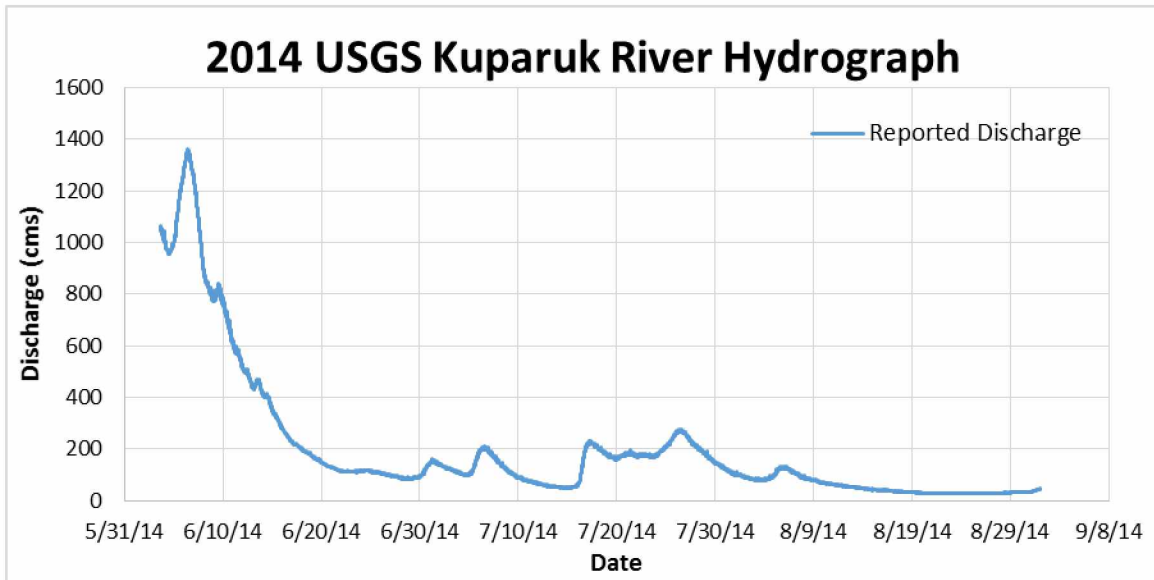
Figure B.21: Hydrograph for the USGS site in 2014.

Hydrograph for the USGS Kuparuk River site as reported by the USGS in 2014.

Appendix C

Appendix C: Calculated lateral inflows for each year at each reach
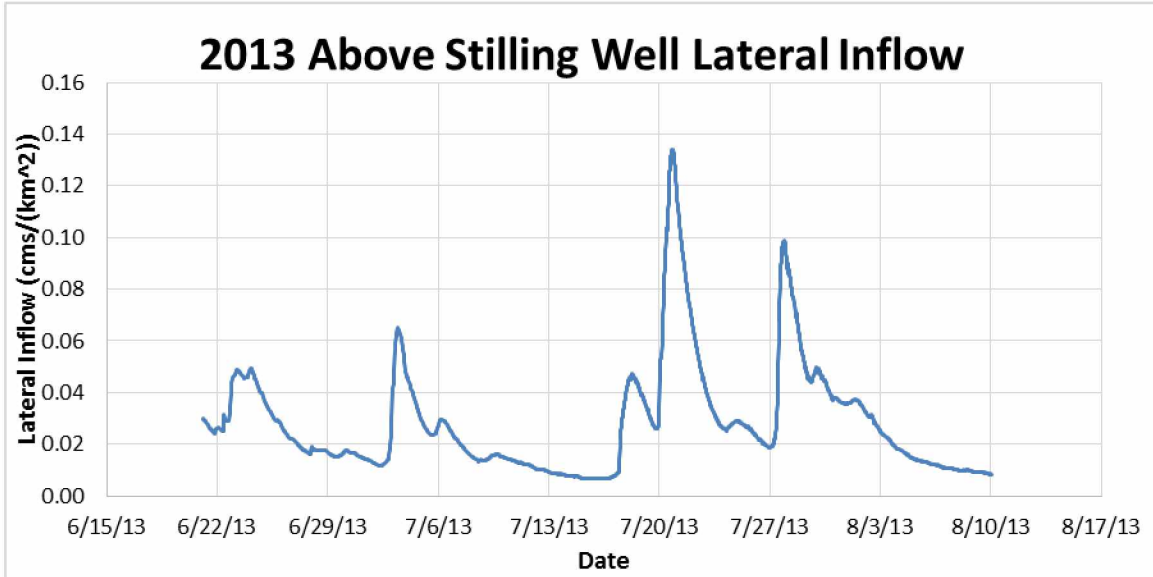
Figure C.1: Calculated lateral inflow for the reach above the Kuparuk River stilling well in 2013.
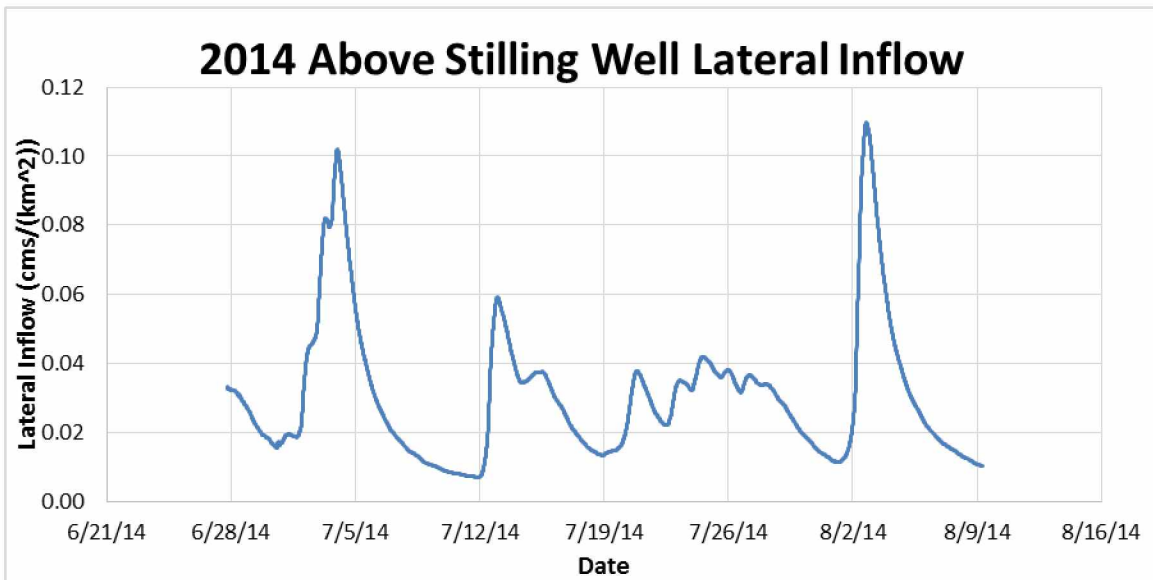
Figure C.2: Calculated lateral inflow for the reach above the Kuparuk River stilling well in 2014.

73
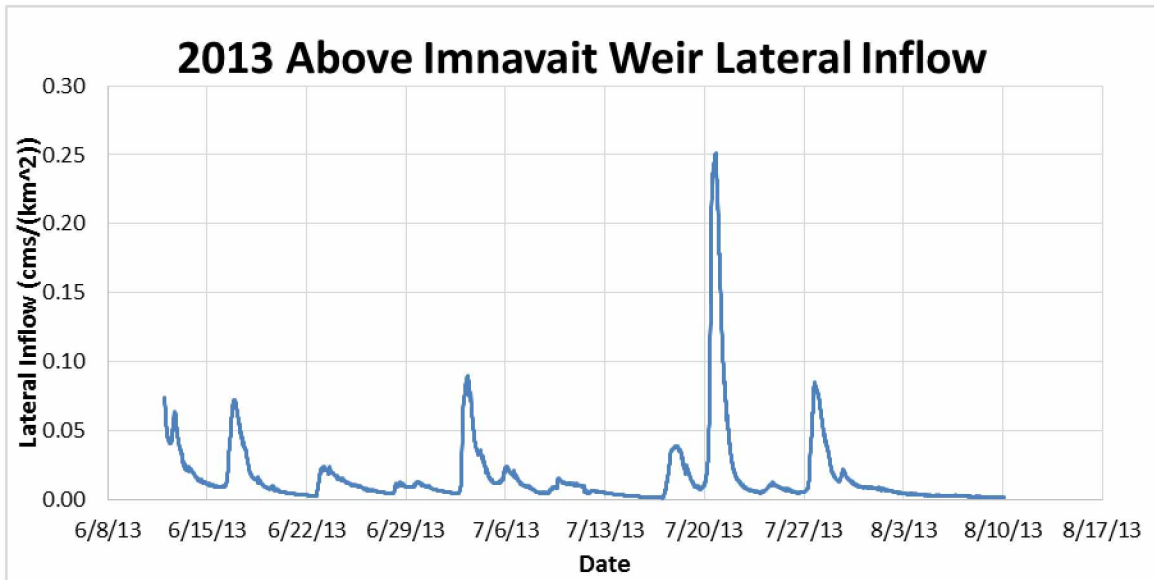
Figure C.3: Calculated lateral inflow for the reach above the Imnavait Creek weir in 2013.
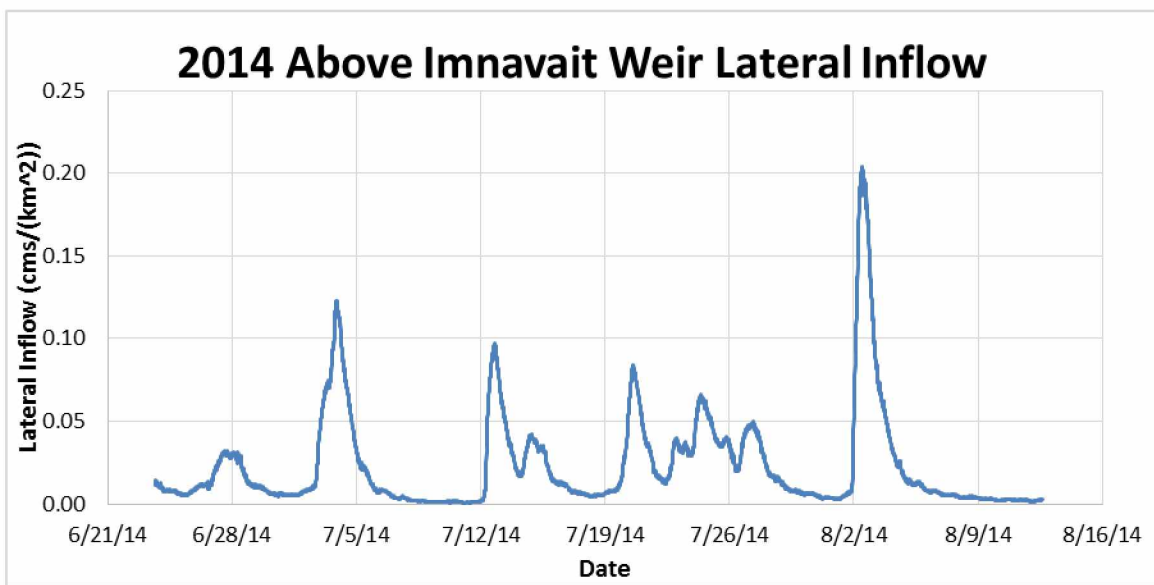
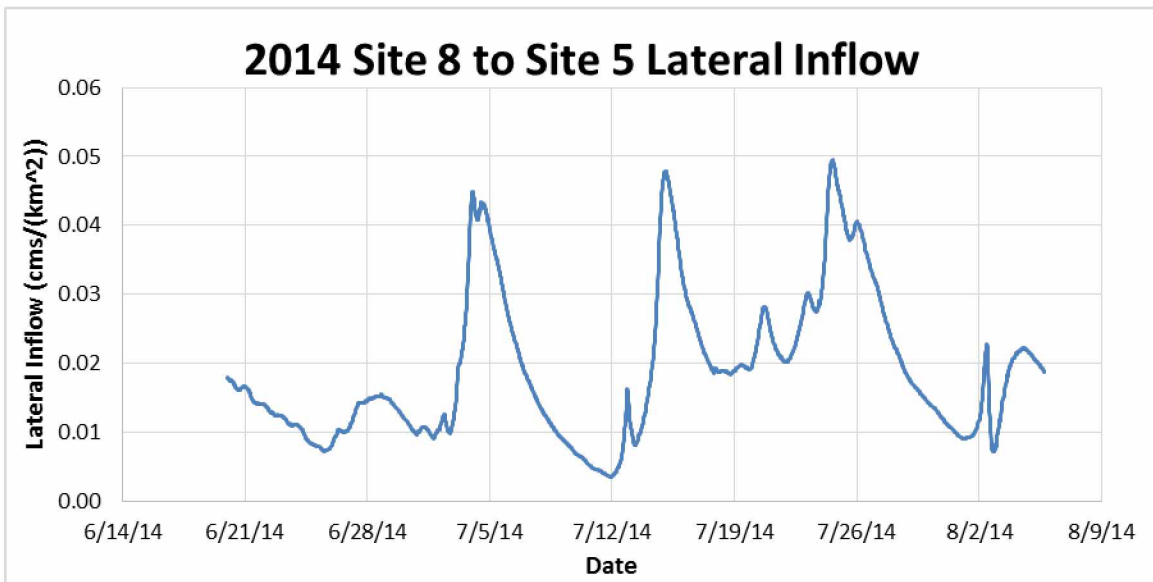
Figure C.4: Calculated lateral inflow for the reach above the Imnavait Creek weir in 2014.
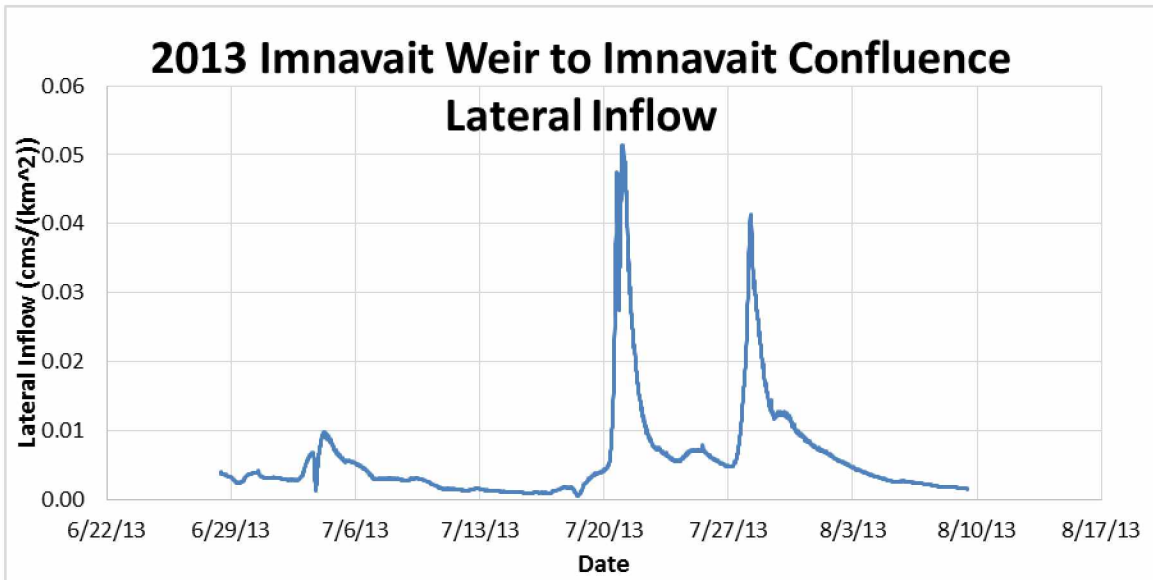
Figure C.5: Calculated lateral inflow for the reach from the Imnavait Creek weir to the Imnavait Creek Confluence in 2013.
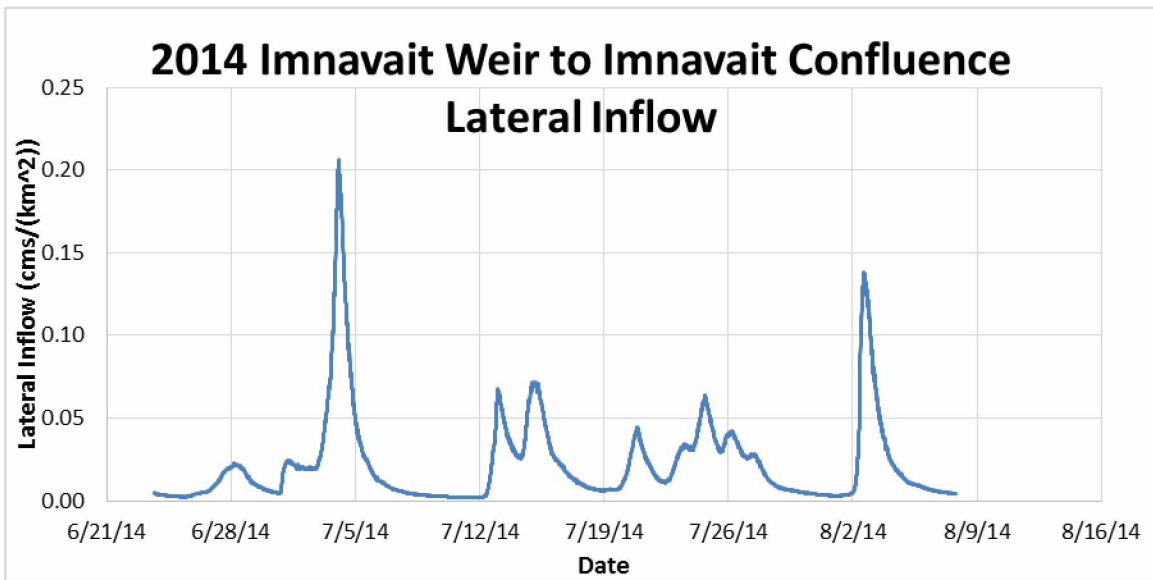
Figure C.6: Calculated lateral inflow for the reach from the Imnavait Creek weir to the Imnavait Creek Confluence in 2014.
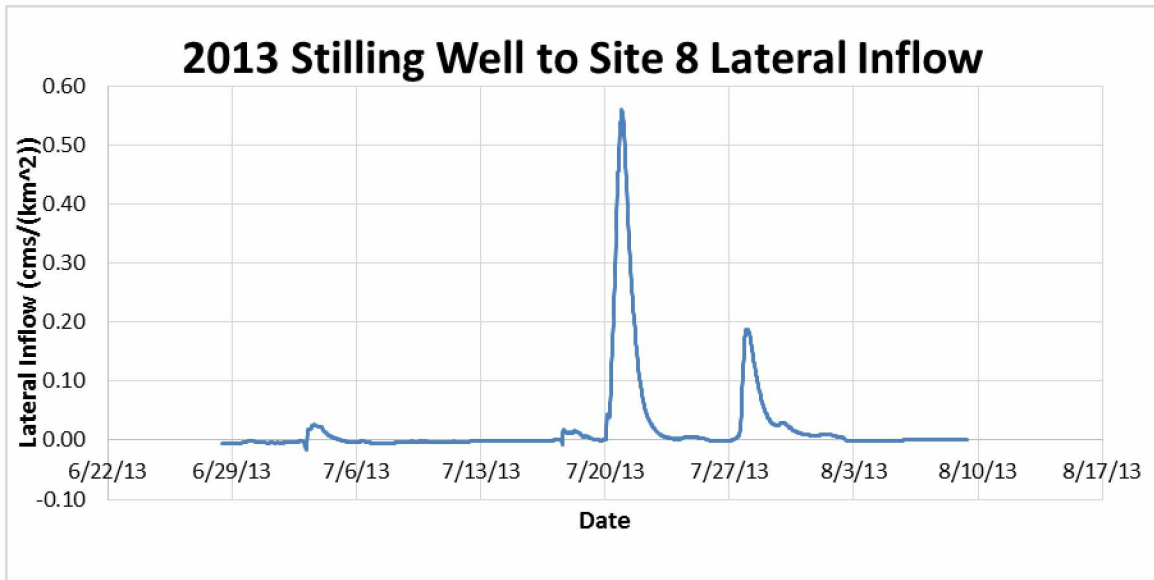
Figure C.7: Calculated lateral inflow for the reach from the Kuparuk River stilling well to site 8 in 2013.
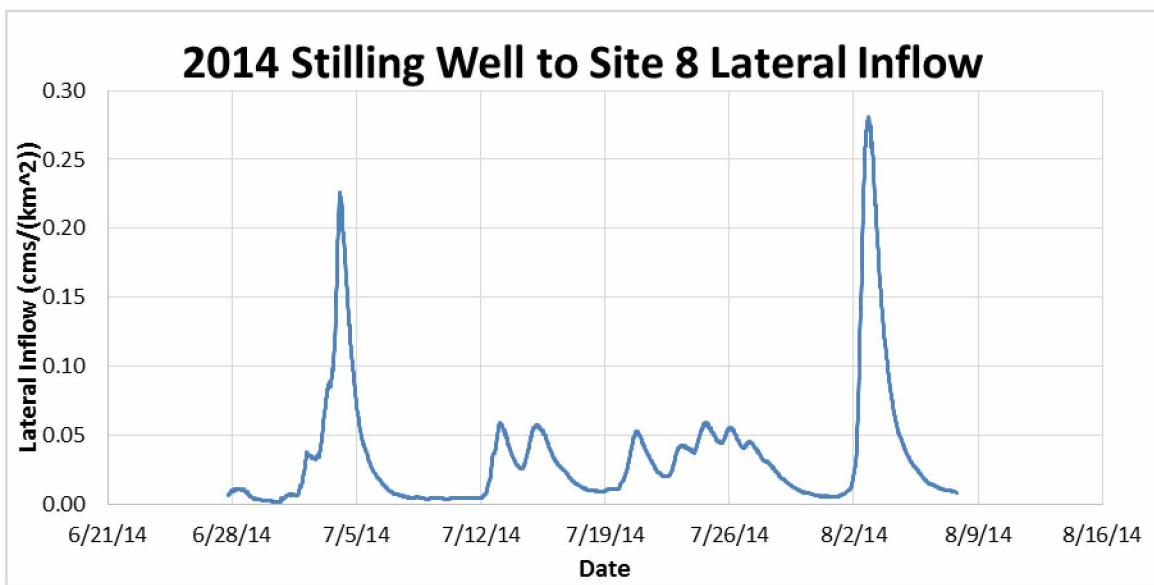
Figure C.8: Calculated lateral inflow for the reach from the Kuparuk River stilling well to site 8 in 2014.
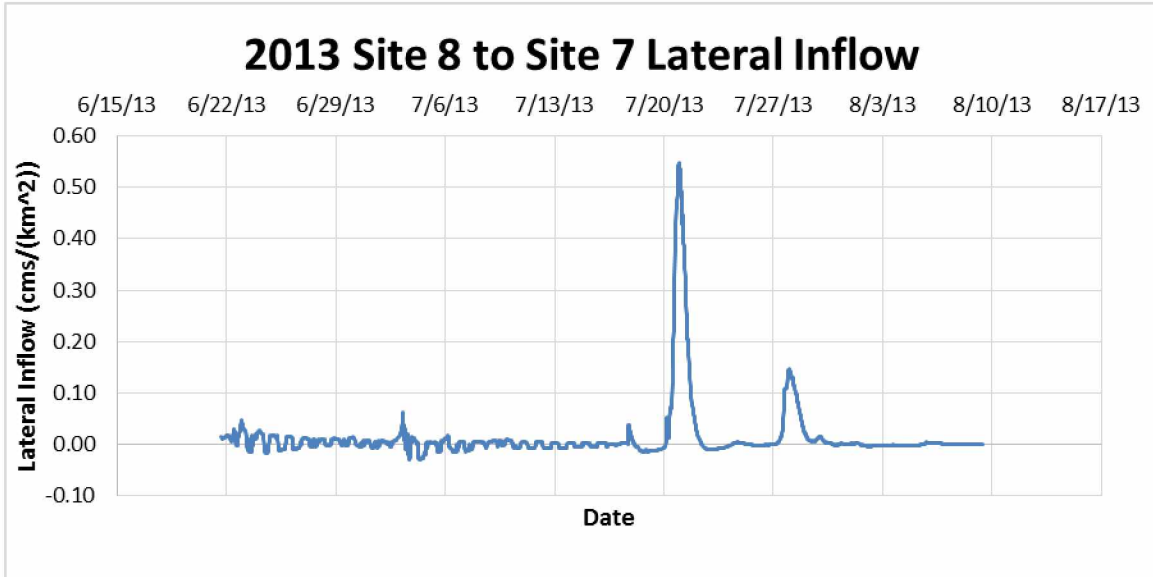
Figure C.9: Calculated lateral inflow for the reach from site 8 to site 7 in 2013.
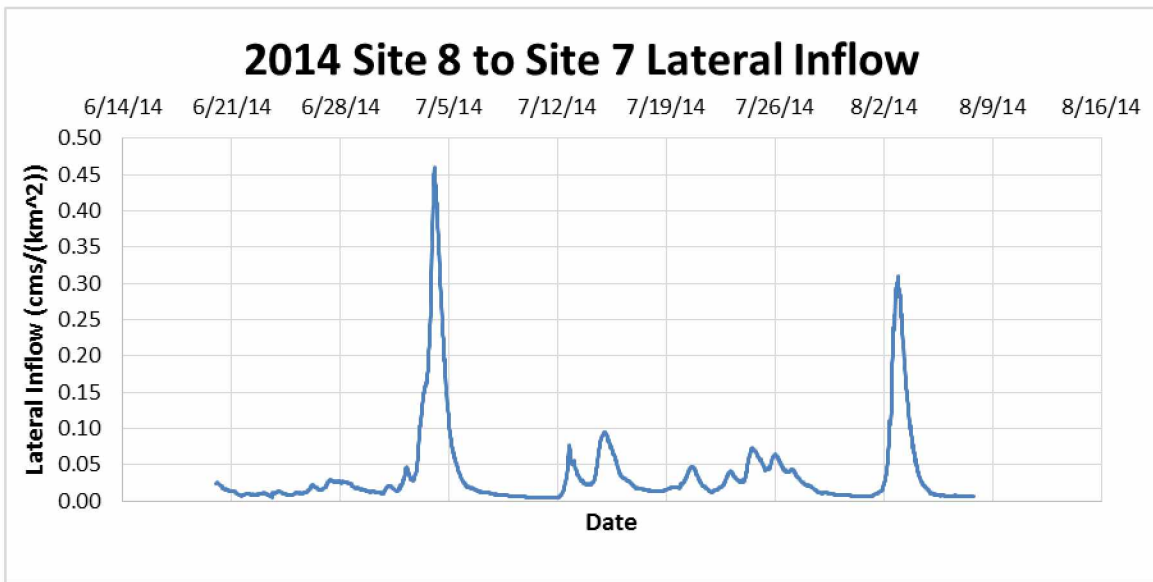
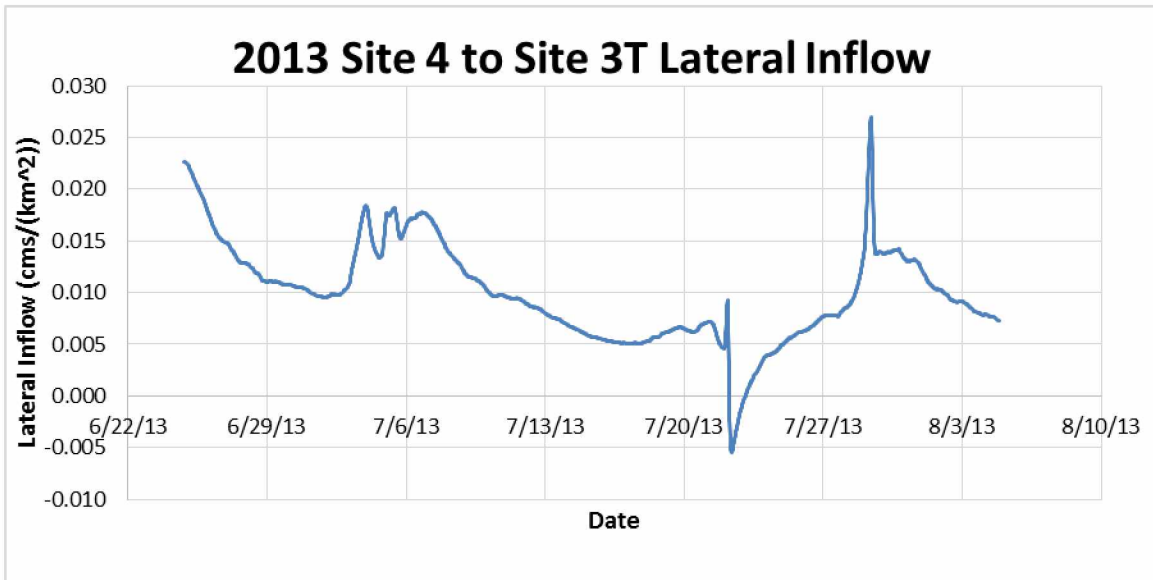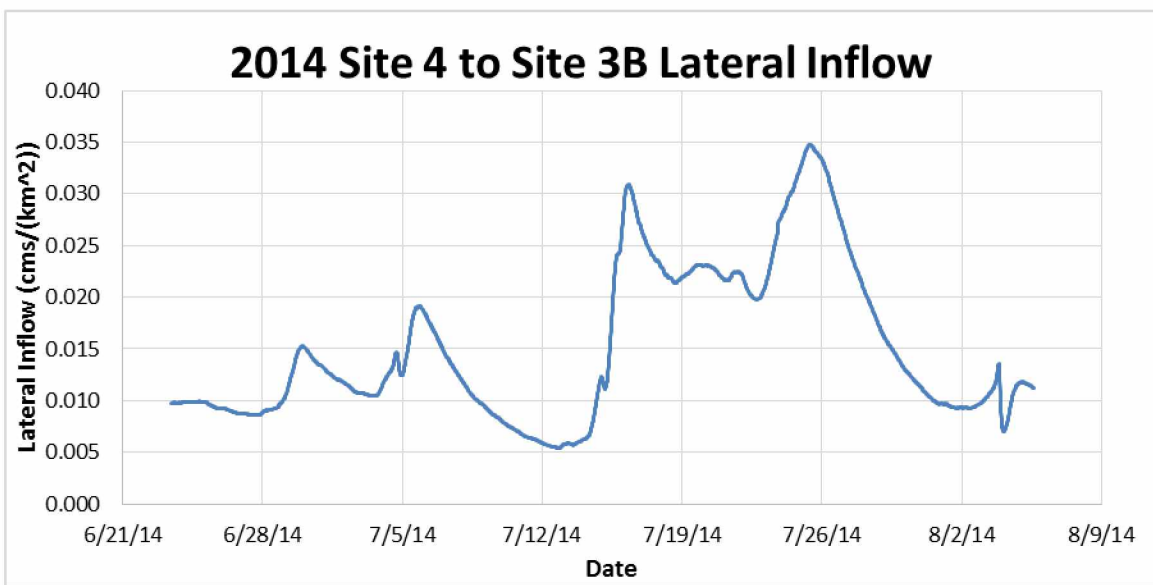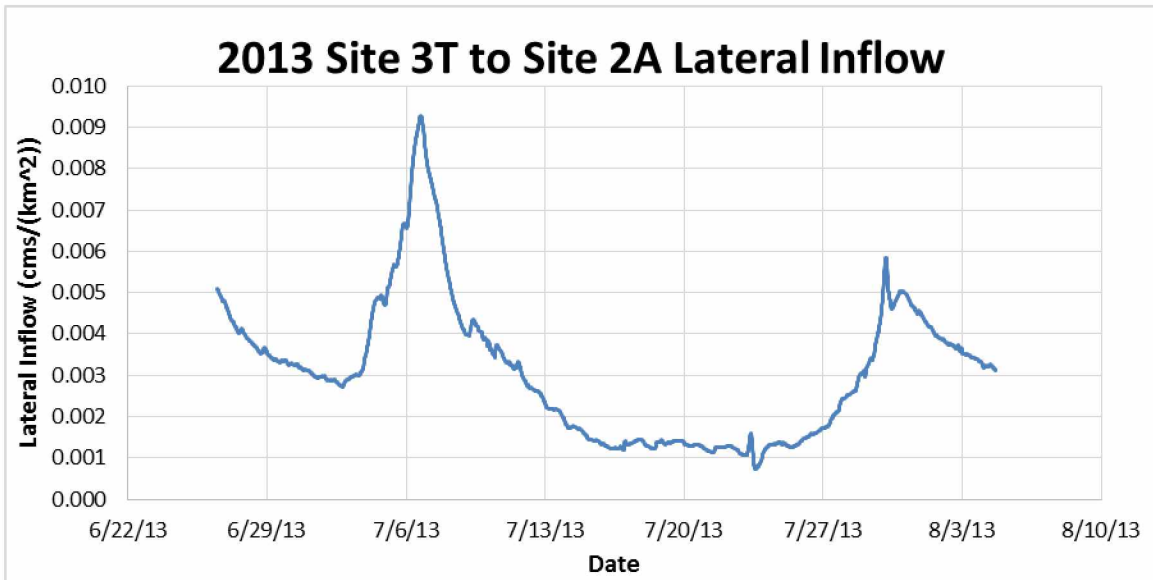Figure C.10: Calculated lateral inflow for the reach from site 8 to site 7 in 2014.
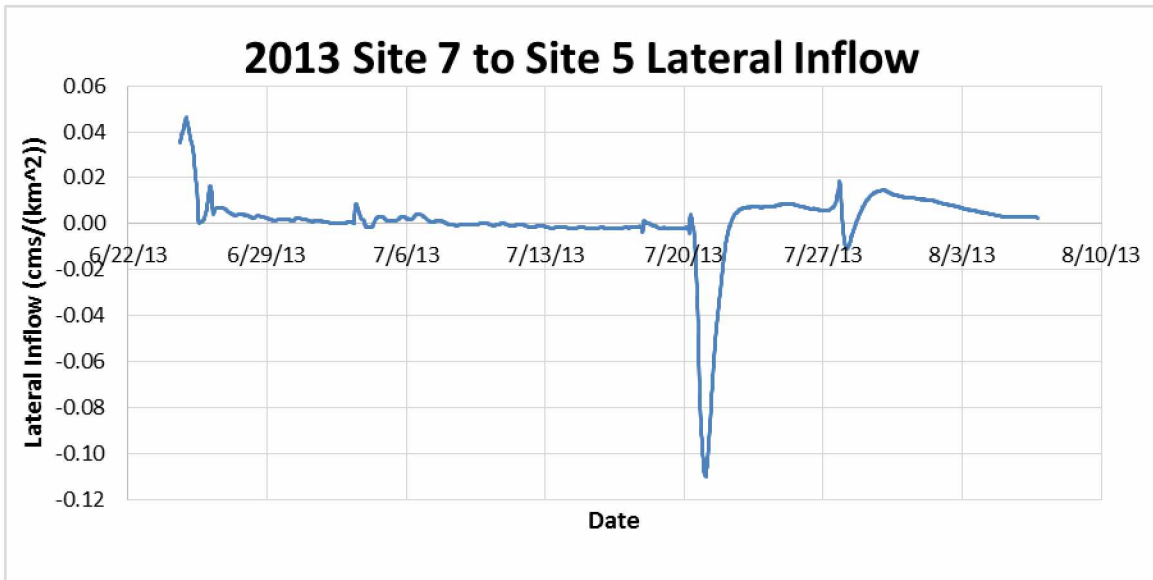
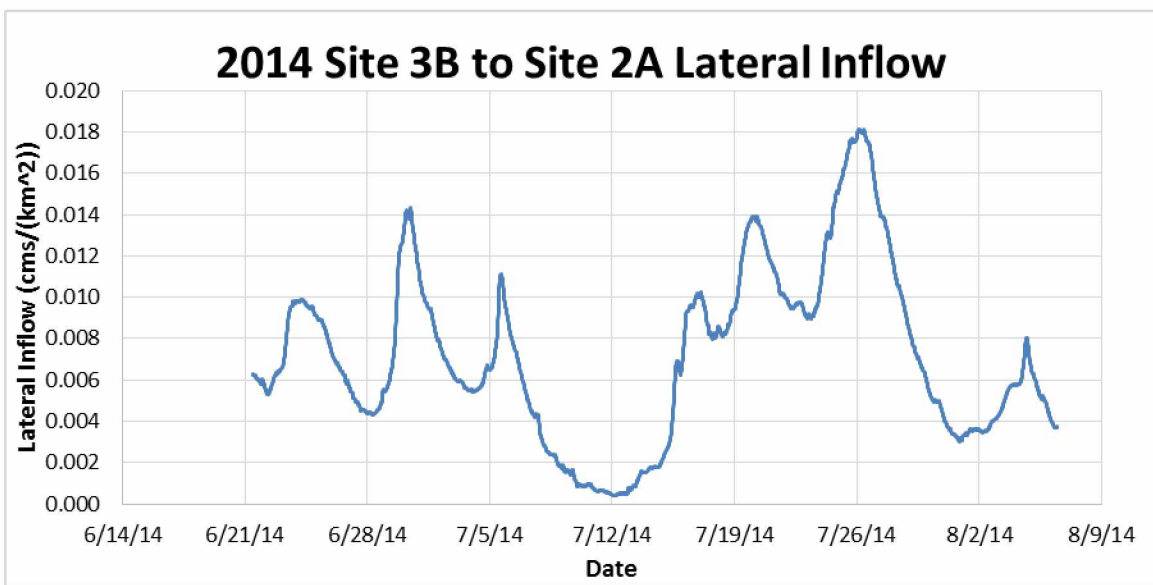Figure C.11: Calculated lateral inflow for the reach from site 7 to site 5 in 2013.
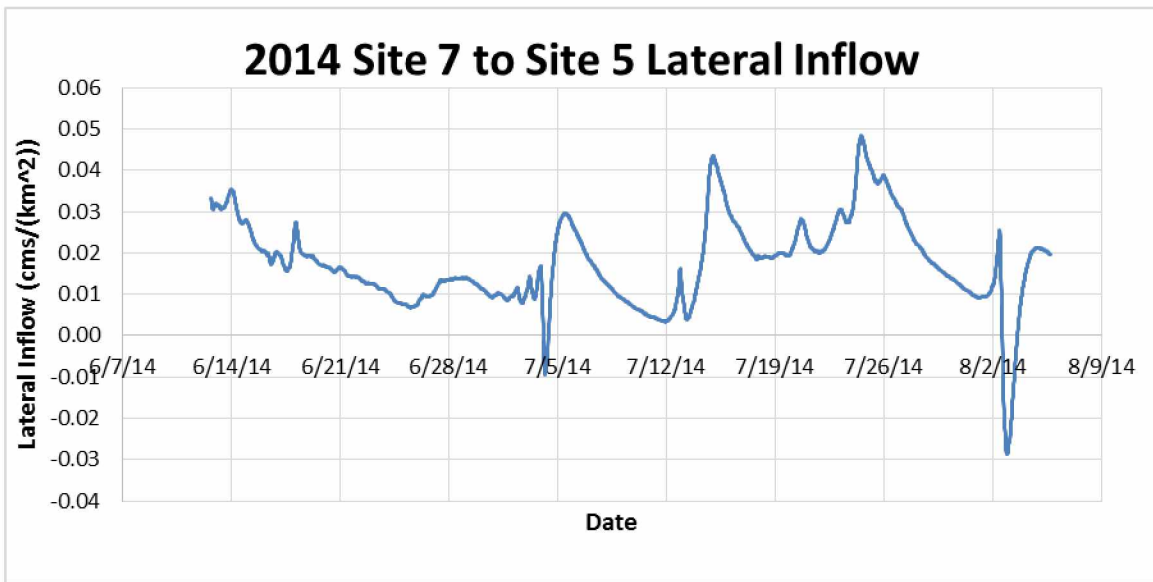
Figure C.12: Calculated lateral inflow for the reach from site 7 to site 5 in 2014.
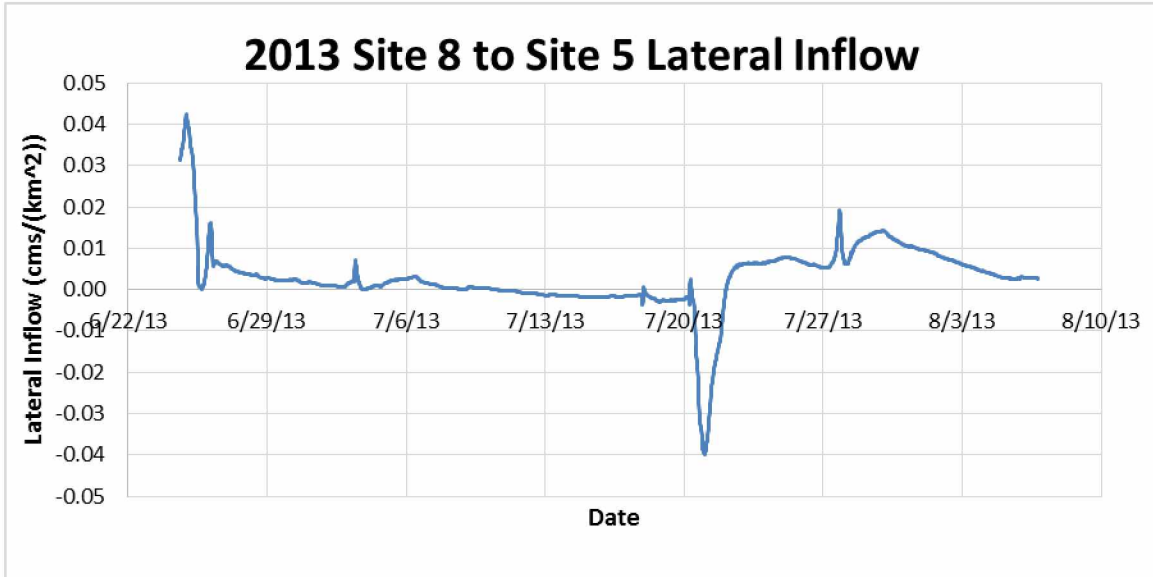
Figure C.13 Calculated lateral inflow for the reach from site 8 to site 5 in 2013

Figure C.14 Calculated lateral inflow for the reach from site 8 to site 5 in 2014.

Figure C.15: Calculated lateral inflow for the reach from site 4 to site 3T in 2013.

Figure C.16: Calculated lateral inflow for the reach from site 4 to site 3B in 2014.

Figure C.17: Calculated lateral inflow for the reach from site 3T to site 2A in 2013.

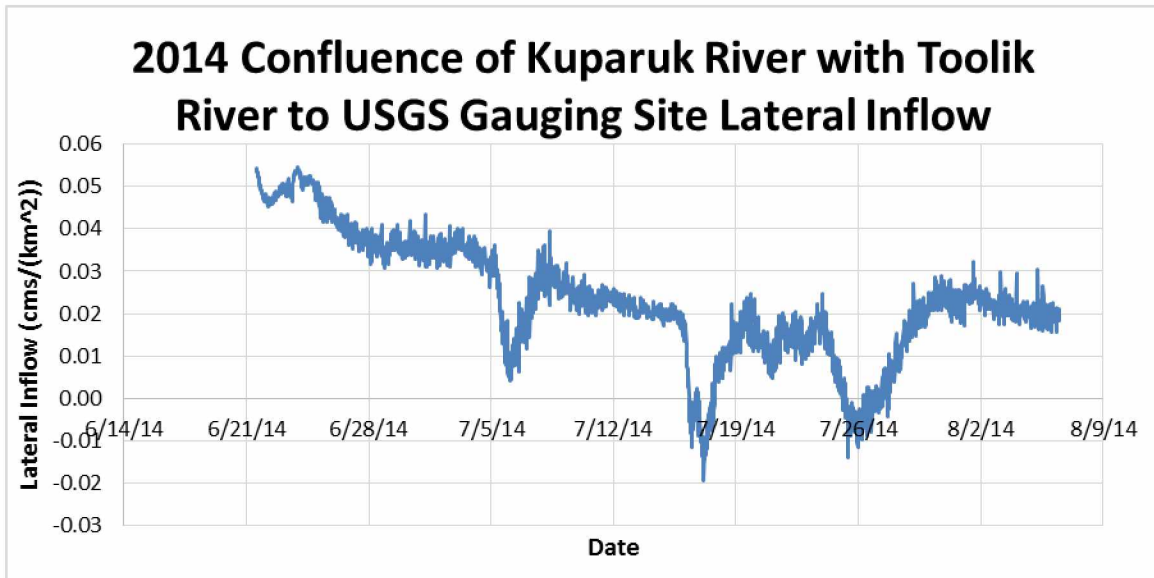Figure C.18: Calculated lateral inflow for the reach from site 3B to site 2A in 2014.

Figure C.19: Calculated lateral inflow for the reach from the confluence of the Kuparuk River with the Toolik River to the USGS gauging site in 2014.

Appendix D: Maps showing the meteorological stations used and their Thiessen polygons
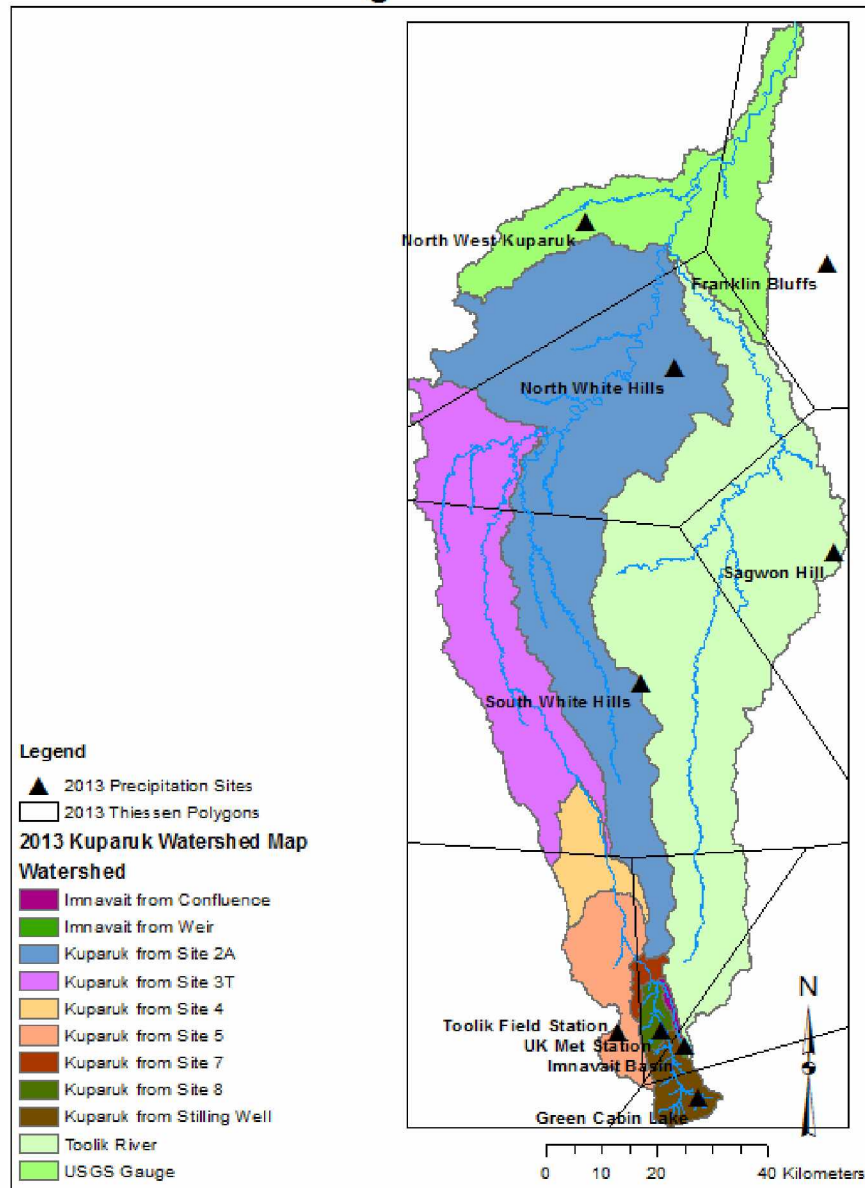

Figure D.1 Map of the Kuparuk watershed showing the meteorological stations used in 2013 and the corresponding Thiessen polygons.
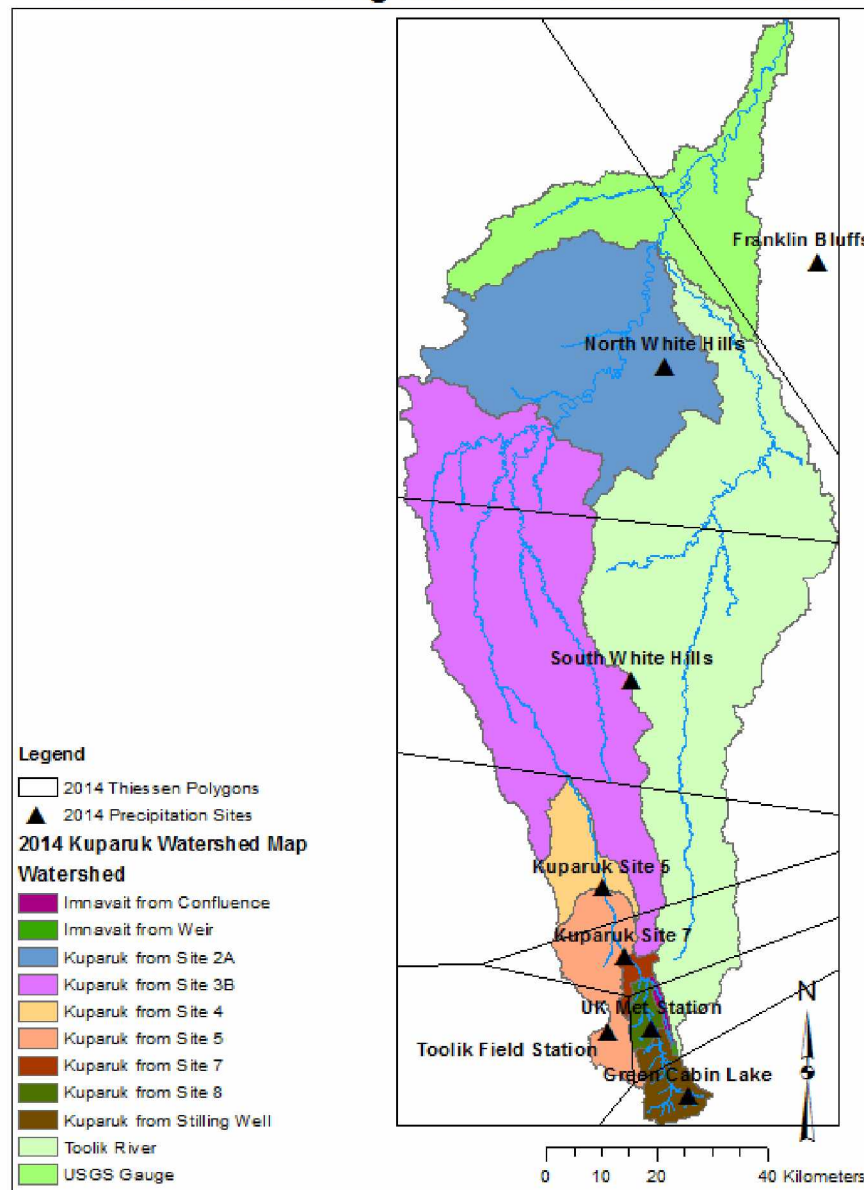
Figure D.2 Map of the Kuparuk watershed showing the meteorological stations used in 2014 and the corresponding Thiessen polygons.